Computational and Structural Biotechnology Journal 19 (2021) 4319–4335

COMPUTATIONAL AND STRUCTURAL BIOTECHNOLOGY JOURNAL

journal homepage: www.elsevier.com/locate/csbj

Chirality affects cholesterol-oxysterol association in water, a computational study

Michal Markiewicz [a,*,1], Robert Szczelina [b], Bozena Milanovic [a], Witold K. Subczynski [c], Marta Pasenkiewicz-Gierula [a,2,*]

[a] Department of Computational Biophysics and Bioinformatics, Faculty of Biochemistry, Biophysics, and Biotechnology, Jagiellonian University, Krakow, Poland
[b] Division of Computational Mathematics, Faculty of Mathematics and Computer Science, Jagiellonian University, 30-348 Krakow, Poland
[c] Department of Biophysics, Medical College of Wisconsin, Milwaukee, WI 53226, USA

ARTICLE INFO

Article history:
Received 17 April 2021
Received in revised form 18 July 2021
Accepted 21 July 2021
Available online 26 July 2021

Keywords:
7α,β-Oxycholesterol
Atherosclerosis
Sterol hydration
Dimerization
Contact area dehydration
Voronoi diagram

ABSTRACT

Cholesterol (Chol) is the most prevalent sterol in the animal kingdom and an indispensable component of mammalian cell membranes. Chol content in the membrane is strictly controlled, although the oxidation of phospholipids may change the relative content of membrane Chol. An excess of it results in the formation of pure Chol microdomains in the membrane. It is likely that some Chol molecules detach from the domains and self-assemble in the aqueous environment. This may promote Chol microcrystallisation, which initiates the development of gallstones and atherosclerotic plaque. In this study, the molecular dynamics, free energy perturbation, umbrella sampling and Voronoi diagram methods are used to reveal the details of self-association of Chol and its oxidised forms (oxChol), namely 7α,β-hydroxycholesterol and 7α,β-hydroperoxycholesterol, in water. In the first part of the study the interactions between a sterol monomer and water over a short and longer timescale as well as the energy of hydration of each sterol are analysed. This helps one to understand Chol-Chol and Chol-OxChol with different chirality self-association in water better, which is analysed in the second part of the study. The Voronoi diagram approach is used to determine the relative arrangement of molecules in the dimer and, most importantly, to analyse the dehydration of the contacting surfaces of the assembling molecules. Free energy calculations indicate that Chol and 7β-hydroxycholesterol associate into the most stable dimer and that Chol-Chol is the next most stable of the five dimers studied. Employing different computational methods enables us to obtain an adequate picture of Chol-sterol self-association in water, which includes dynamic, energetic and temporal aspects of the process.

1. Introduction

One of the central processes in biology is the assembly of biomolecules into organised structures. An important driving force in this process is the hydrophobic effect. Its organisational power reveals itself when amphiphilic molecules added to water self-associate to form structured aggregates.

Cholesterol (Chol, Fig. 1), the most prevalent sterol in the animal kingdom, plays important physiological and physicochemical roles in the human body, but also participates in the pathologic processes of the formation of gallstones and atherosclerotic plaques. Both of these processes are related to highly elevated Chol levels and involve the formation of Chol microcrystals [1–4]. In this formation cholesterol crystal nucleation is a critical initial phase [1,2] as it is the first step in the emergence of a new structure via self-assembly and self-organisation.

Chol is amphiphilic and in a polar solvent (water) its molecules self-assemble. Self-assembly is a rapid process, whereas self-organisation is a significantly slower one. The activity of Chol in water was intensively studied in the 1970s, e.g. [5–7]. These studies indicated that at very low Chol concentrations Chol micelles and Chol monomers are in a reversible equilibrium, the critical micelle concentration is exceptionally low, 25–40 nM at 25°, and the total solubility of Chol in water is 4.7 μM [5]. They also indicated that Chol micelles are stabilised by intermolecular attractive

* Corresponding authors.
E-mail addresses: m.markiewicz@uj.edu.pl (M. Markiewicz), marta.pasenkiewicz-gierula@uj.edu.pl (M. Pasenkiewicz-Gierula).
[1] ORCID ID: 0000-0002-7159-9343.
[2] ORCID ID: 0000-0001-5328-5685.

https://doi.org/10.1016/j.csbj.2021.07.022

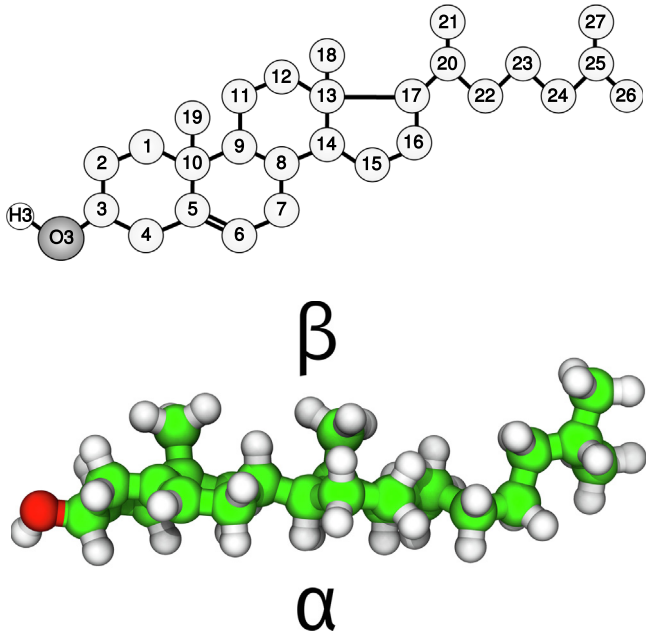

Fig. 1. Molecular structure of Chol. (Upper) The Chol atoms in the scheme are numbered according to the IUPAC convention [19]. The chemical symbol for carbon atoms, C, is omitted and the hydrogen atoms are not shown except for the Chol OH group, where the H atom is explicitly included. (Lower) The 3D structure of Chol with the smooth α- and the rough β-face marked.

forces in addition to hydrophobic repulsion by the solvent and that Chol hydrophobicity is much less than theoretically predicted [6].

When the Chol content in a phospholipid (PL) bilayer exceeds saturation limit [8], pure Chol cross-bilayer domains (Chol bilayer domain, CBD) are formed [8–12]. However, pure Chol bilayers have not been detected as thermodynamically stable spontaneously formed Chol aggregates in water, though they possibly exist [13]. The final form of a Chol aggregate in water, obtained in a long process of self-organisation, is a monohydrate crystal [7,14]. In terms of its structure, a Chol monohydrate crystal consists of a very large number of structurally ordered bilayers stacked on top of each other [15–16], where Chol molecules are cross-linked by hydrogen bonded (H-bond) water molecules and by direct Chol···Chol H-bonds [15]. However, pre-crystal aggregates that form in water as well as CBDs are far more hydrated than monohydrate crystal, e.g. [17,18]. On average, each Chol molecule in the CBD makes H-bonds with 2.3 water molecules [18].

Pathologic processes involving Chol that occur in the human body and particularly those leading to atherosclerotic plaque formation are promoted by two main factors, which are a high Chol content in the plasma membranes of the arterial cells and oxidative stress, which can lead to phospholipid peroxidation. The initiation of the atherosclerotic process is related to the crystallisation of free Chol [4,20]. The possible sources of free Chol in the initial stages of atherosclerotic plaque formation are discussed in our previous paper [21]. In brief, one of the sources might be oxidised low-density lipoproteins; the other Chol domains in plasma membranes oversaturated with the Chol of the arterial wall cells. The process involving the former source has been widely studied and discussed in the literature and it seems to be well established [22,23]. The latter has been postulated recently e.g. in Refs [9,12,21] and the hypothesis has been put forward that a Chol membrane domain, as a whole, may disconnect from the membrane and collapse in the form of a Chol seed crystal [21]. This paper is based on the third possibility, which assumes that a Chol crystal nucleation starts outside a Chol oversaturated membrane. From such a membrane, where the molar ratio of Chol to PL is ~ 2:1, individual Chol molecules may detach and self-associate in the aqueous phase. The possible role of oxidative stress in this process is significant as it generates phospholipid peroxidation, which in the case of polyunsaturated acyl chains introduces a hydroperoxide group into the chain at a double-bond position. This may trigger chain fragmentation giving rise to truncated chains with polar groups at their ends [24–27], loosening the packing of the lipids and severely destabilising the membrane. This possibly will facilitate detachment of individual Chol molecules from the membrane, their self-association in the aqueous phase and the eventual formation of a Chol crystal nucleus.

The self-assembly of Chol molecules outside the membrane, which might eventually lead to the formation of microcrystals that initiate pathologic processes in the human body [1–4], have not been studied yet. The aim of this study is to elucidate how Chol nucleation proceeds in water and how different oxidised forms of Chol (oxysterols, oxChols) can affect it. The research was carried out in model systems using computational methods.

However, before elucidating how the initial stages of Chol and oxChols association in water might proceed, it is necessary to indicate and characterise the basic interactions between Chol and water, oxChol and water as well as the details of the formation of Chol-Chol and Chol-oxChol dimers (primary nucleation [28,29]) in water. These issues are the subject of this paper.

The oxidised forms of Chol investigated are 7α- and 7β-hydroxycholesterol (7α-OH-Chol, 7β-OH-Chol), and 7α- and 7β-hydroperoxycholesterol (7α-OOH-Chol, 7β-OOH-Chol) (Figs. 2 and S1, Supporting Information, SI). 7-OH-Chol and 7-OOH-Chol have been chosen because they are among the major products of Chol oxidation [30]. As 7β-OH-Chol and 7β-OOH-Chol rather than 7α-OH-Chol and 7α-OOH-Chol are found in the early and advanced stages of human atherosclerotic plaques [31–34], it is thus important to elucidate the effect of oxysterol chirality on the formation and stability of Chol aggregates in water.

2. Materials and methods

In this study, both the dynamics and the energetics of the interactions of Chol and oxChol molecules with water as well as Chol-Chol and Chol-oxChol self-associations in water were analysed using classical molecular modelling with atomic resolution and 3D Voronoi diagrams. To investigate the dynamics, molecular dynamics (MD) simulation was used. To assess energetics, free energy perturbation (FEP) and umbrella sampling (US) methods were employed. These calculations were carried out using the package GROMACS [35,36].

2.1. Simulation systems parameters and conditions

2.1.1. Simulation parameters

For the Chol and oxChol molecules, all-atom optimised potentials for liquid simulations (OPLS-AA) [37] were used. The atomic charges on each sterol molecule were calculated using the Restrained Electrostatic Potential (RESP) method [38], and are given in Table 1 (Data in Brief, Markiewicz et al., XXXX). The missing torsional parameters for the hydroperoxy group of 7-OOH-Chol were obtained by fitting to the rotational profile calculated for 36 rotamers using Hybrid Methods for Interaction Energies [39,40] (details are given in Data in Brief, Markiewicz et al., XXXX), and are given in Table 2 (Data in Brief, Markiewicz et al., XXXX). For water, the transferable intermolecular potential three-point model (TIP3P) was employed [41]. The linear constraint solver (LINCS) algorithm [42] was used to preserve the length of every covalent bond with a hydrogen atom with LINCS order of 4 (for MD and

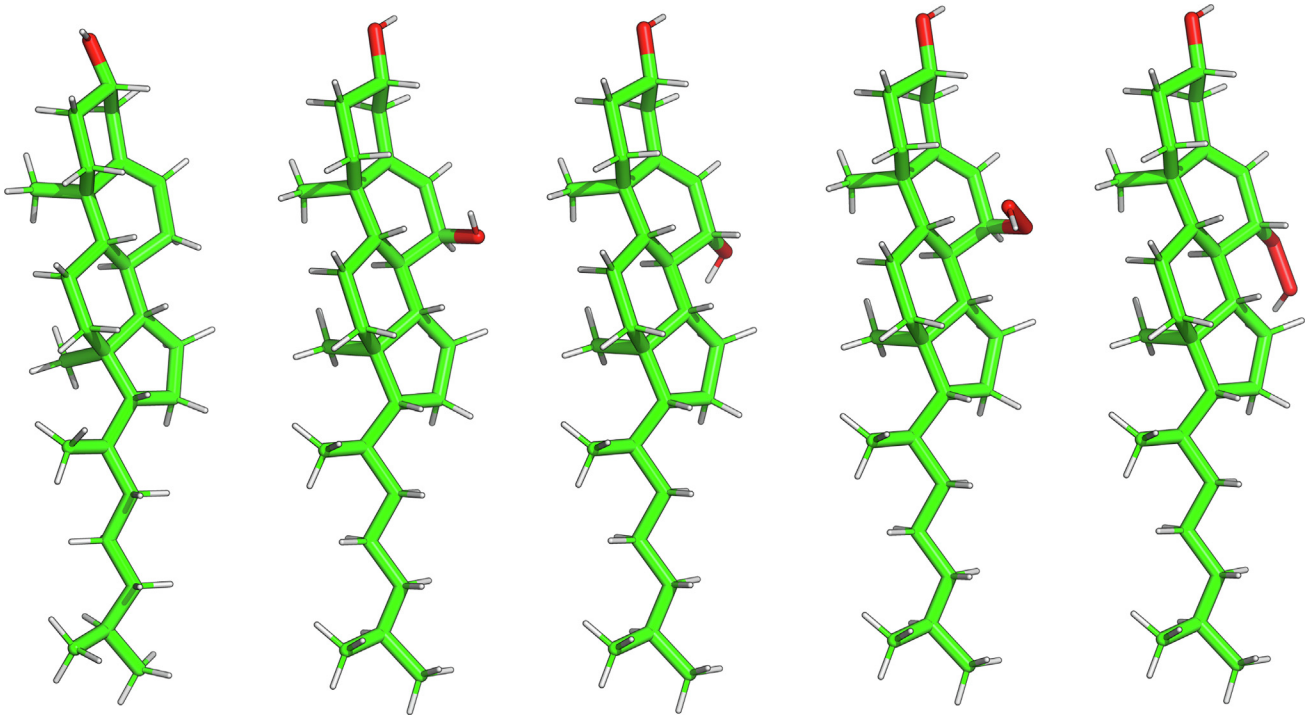

Fig. 2. Three-dimensional structures of Chol and oxidised forms of Chol. From left to right: Chol, 7α-OH-Chol, 7β-OH-Chol, 7α-OOH-Chol, 7β-OOH-Chol. The atoms are represented in standard colours.

Table 1
Average *L1* water- sterol distance (Sterol-water distance) and sterol volume (Sterol volume).

Sterol	Sterol volume [Å^3]	Sterol-water distance [Å]
Chol	561.66 ± 16.65	4.18 ± 0.09
O7a	571.10 ± 17.63	4.16 ± 0.10
O7b	569.99 ± 18.25	4.16 ± 0.10
OO7a	590.10 ± 15.61	4.12 ± 0.09
OO7b	598.17 ± 17.04	4.17 ± 0.09

The time average (between 10 and 100 ps) *L1* water-sterol distance and the volume available to the sterol molecule for Chol; 7α-OH-Chol (O7a); 7β-OH-Chol (O7b); 7α-OOH-Chol (OO7a); 7β-OOH-Chol (OO7b) in water. Abbreviations used in the Table are explained in the text (α (a) and β (b) are chiral forms of the hydroxy and hydroperoxy groups, '7' refer to the C7 carbon atom of the sterol molecule, cf. Fig. 1).

US calculations) and 12 (for FEP calculations), and the time step was set to 2 fs.

The van der Waals (vdW) interactions were cut off at 1.0 nm (for MD simulations), 1.2 nm (for FEP calculations) and 1.4 nm (for US calculations). Long-range electrostatic interactions were evaluated using the particle-mesh Ewald summation method with a β-spline interpolation order of 5 and direct sum tolerance of 10^{-5} [43]. For the real space, a cut off of 1.0 nm (for MD simulations), 1.2 nm (for FEP calculations) and 1.4 nm (for US calculations), three-dimensional periodic boundary conditions, and the minimum image convention were used. The higher cut off values for FEP calculations were used to minimize errors in the Gibbs free energy associated with truncating the long-range electrostatic interaction, and for US calculations to increase the readability of the potential of mean force plots.

2.1.2. Simulation conditions

Unrestrained MD simulations were carried out in the *NVT* ensemble (the number of particles, *N*, system volume, *V*, and temperature, *T*, constant) at a physiological temperature 310 K. The temperatures of the solute and solvent were controlled independently using the Berendsen method [44] with a relaxation time of 0.6 ps. The list of nonbonded pairs was updated every five steps (10 fs).

Free energy perturbation and umbrella sampling calculations were carried out in the *NTp* ensemble (the number of particles, *N*, system temperature, *T*, pressure, *p*, constant) at a physiological temperature 310 K (37 °C) and pressure of 1 atm. The temperatures

Table 2
Average energies of sterol-water and water-water interactions.

	Energies [kcal/mol]			
Sterol	Coulomb sterol-water	vdW sterol-water	Coulomb water-water	vdW water-water
Chol	−15.3 ± 3.9	−31.9 ± 3.0	−23265.8 ± 95.7	3205.0 ± 67.5
O7a	−25.5 ± 5.0	−31.2 ± 3.3	−23181.9 ± 113.0	3185.8 ± 74.5
O7b	−26.5 ± 5.2	−30.5 ± 3.4	−23228.1 ± 103.7	3198.3 ± 69.7
OO7a	−28.2 ± 5.2	−31.2 ± 3.2	−23176.9 ± 101.9	3189.1 ± 70.1
OO7b	−25.6 ± 5.2	−30.7 ± 3.2	−23194.5 ± 103.3	3193.0 ± 71.5

The time average (between 10 and 100 ps) energies of sterol-water and water-water Coulomb and vdW interactions for Chol; 7α-OH-Chol (O7a); 7β-OH-Chol (O7b); 7α-OOH-Chol (OO7a); 7β-OOH-Chol (OO7b) in water. Abbreviations used in the Table are explained in the text (α (a) and β (b) are chiral forms of the hydroxy and hydroperoxy groups, '7' refer to the C7 carbon atom of the sterol molecule, cf. Fig. 1).

of the solute and solvent were controlled independently using the Nosé-Hoover method [45,46] with a relaxation time of 0.6 ps. Pressure was controlled anisotropically by the Parrinello-Rahman method [47] with a relaxation time of 1.0 ps.

2.2. Unrestrained MD simulation

Each simulation system consisted of one or two sterol molecules, previously pre-equilibrated in 100-ps MD simulation in water, placed in a water box ($40 \times 40 \times 40$ Å^3) containing ~ 2000 water molecules (water density ~ 1 g/cm^3). The systems were MD simulated for 10 ns using the package GROMACS 5.2 [36].

2.2.1. Sterol-water interaction

To study sterol-water interactions, a Chol monomer or a monomer of each of its four oxidation forms (7α-OH-Chol, 7β-OH-Chol and 7α-OOH-Chol, 7β-OOH-Chol) was placed in a water box and MD simulated. The first 100 ps of the generated trajectory was recorded every 2 fs, from 100 ps to 5 ns, every 400 fs, afterwards every 1.2 ps.

2.2.2. Sterol-sterol interaction in water

Of the two sterol molecules placed in a water box and MD simulated one was Chol, the other was Chol or one of the four oxChols. The initial distance between the centres-of-mass (CM) of the sterol molecules was 10 Å. Each generated trajectory was recorded every 1.2 ps.

2.3. Energy calculations

2.3.1. Free energy perturbation

The FEP method was used to assess the energy of sterol hydration. The energy of hydration is the free energy change when a solute molecule is transferred from vacuum to water. Hydration is understood as a stabilising interaction of a solute with a solvent [48] and involves mainly such interactions as hydrogen (H-) bonding and electrostatic and vdW interactions. Thus, hydration relates to both a soluble and an insoluble material [48].

In this free energy calculation [49], the systems consisting of a $50 \times 50 \times 50$ Å^3 water box containing a Chol or oxChol monomer and ~ 4000 water molecules were used (basic concepts of the free energy method are in SI). Decoupling of the sterol interactions with water molecules is carried out in 30 steps: the first 10 steps decouple the Coulomb interaction; the following 20 steps decouple the vdW interactions. For the latter the soft-core potential was applied with the α parameter of 0.5, the power of λ of 1 and the power of the radial term of 6.

For each λ, the same computational procedure is applied, 1) system optimisation involving 5000 steps of the steepest descent energy minimisation, followed by 5000 steps of L-BFGS (quasi-Newton optimisation algorithm) [50]; 2) system equilibration involving 100-ps MD simulation at a constant volume and 100-ps MD simulation at a constant pressure of 1 atm; 3) 1-ns production MD simulation at 310 K in the *NTp* ensemble. The free energy change is calculated using the Bennett Acceptance Ratio method [51] implemented in the package GROMACS 2016.

2.3.2. Umbrella sampling

The free energy of the association of two sterol molecules in water was calculated from the free energy profile along a reaction coordinate obtained from US simulations [52]. Here the reaction coordinate is the distance between the C13 carbon atoms (Fig. 1) of the associating molecule (Chol or oxChol) and the target (Chol) (C13-C13 distance).

To determine the starting configurations for umbrella sampling windows, the associating molecule was pulled towards the target in a steered MD (SMD) simulation [53]. In this 5.5-ns SMD simulation, the harmonic potential with the spring constant of 1000 kJ/(mol·nm^2) was assigned to the C13 carbon atom of the associating molecule (Fig. 1) and the molecule was pulled at a constant velocity of 0.0003 nm/ps (0.3 nm/ns) along the reaction coordinate. From the trajectory generated in SMD simulation, 70 starting configurations were selected for the US simulations. For each window, MD simulation with harmonic bias potential (US simulation) with a spring constant of 1000 kJ/(mol·nm^2) was carried out for 10 ns and preceded by 100-ps system equilibration.

The weighted histogram analysis method (WHAM) [54] implemented in the package GROMACS was used to analyse the free energy change on the association of sterol molecules in water. A Bayesian bootstrap analysis and 500 bootstrap profiles (Fig. S2b, SI) were used to calculate the average energy profile and mean square displacements. From the profile, the average free energy change and its standard deviation were obtained.

To calculate the free energy of the dimer formation, a system consisting of two sterol molecules in a $40 \times 40 \times 40$ Å^3 box filled with ~ 2000 H_2O molecules was used. Initially, the sterol molecules were separated by ~ 18 Å. Both molecules were positionally unrestrained and free to move with only the C13-C13 distance constrained.

Each sterol molecule used in US simulations had been previously pre-equilibrated in 100-ps MD simulation in water in the *NTp* ensemble.

2.4. Analyses

The interactions between a sterol monomer and water molecules were assessed for two time periods, during the first 100 ps of MD simulations to evaluate the system equilibration and at equilibrium (beyond 100 ps); also by calculating the free energy of sterol hydration.

When evaluating the association of sterol molecules in water, special attention was paid to the time scale, dehydration of the contacting surfaces of the sterol molecules on association, geometry and stability of the dimer that formed and the free energy of association.

2.4.1. Voronoi diagram

The Voronoi diagram is frequently used to find near-neighbour objects to a given object (basic definitions and properties of the Voronoi diagram are in SI and depicted in Figs. 3 and 4). In this study, the Voronoi diagram is applied to analyse the hydration of sterol molecules in water, the geometric properties of sterol dimers formed in water and the behaviour of the water between two sterol molecules during their association.

2.4.1.1. Sterol hydration. To analyse sterol-water interactions, the systems described in Section 2.2.1 were used. To monitor equilibration processes of the systems, for the first 50,000 frames (equally spaced in time by a 2-fs interval) of each generated trajectory, a 3D Voronoi diagram was constructed using the Python package DMG-α [55]. To speed up computations, the sites/objects of the Voronoi diagram comprised only the heavy atoms of sterol and water. For more information cf. SI. The sterol-water interactions at equilibrium (long-term) were analysed in an analogical way.

The first hydration layer (*L1*) of sterol was defined as all water molecules whose Voronoi cells were neighbours of the sterol Voronoi cells. The second hydration layer (*L2*) was a set of water molecules whose Voronoi cells were neighbours of the *L1*. Layers *L3*, *L4*, and so on were defined in an analogical way (Fig. 4). The number of

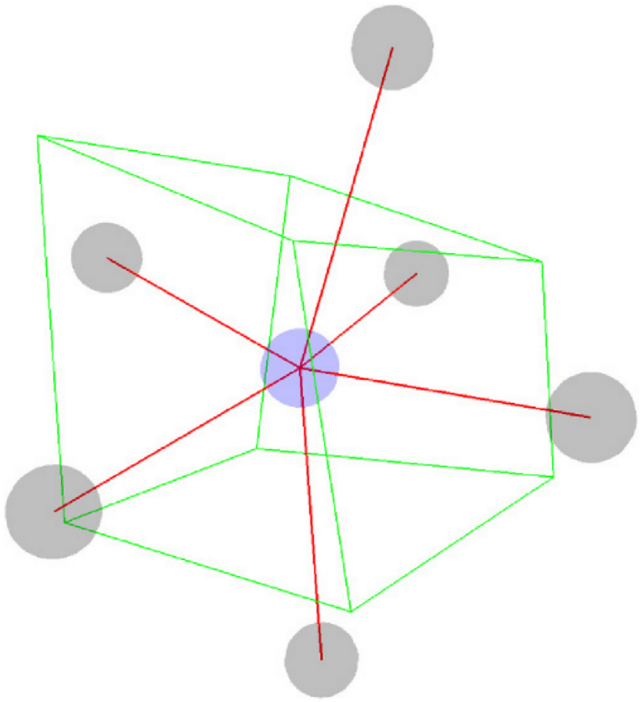

Fig. 3. 3D Voronoi cell (green lines) of the middle (blue) site. In the example, the faces of the Voronoi cell (sides) are polygons enclosed by four pairwise intersecting lines. (For interpretation of the references to colour in this figure legend, the reader is referred to the web version of this article.)

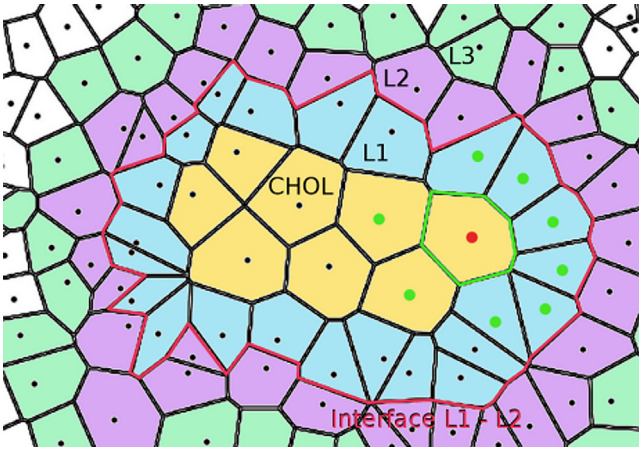

Fig. 4. Schematic 2D depiction of Voronoi cells, sides, neighbours, hydration layers, and boundaries for an imaginary molecule, called here CHOL, immersed in water. All neighbours of the red dot are marked as green dots. The sides of the Voronoi cells neighbouring the red dot are green. Hydration layers *L1*, *L2*, *L3* are blue, violet and green, respectively. The boundary between layers *L1* and *L2* is shown as a red line. (For interpretation of the references to colour in this figure legend, the reader is referred to the web version of this article.)

water molecules in each water layer corresponded to the number of Voronoi cells forming the layer. The layers were constructed using an algorithm similar to the Breadth First Search (BFS) algorithm in Graph Theory [56].

2.4.1.2. Water between two aggregating sterol molecules. When two sterol molecules in water approach each other to eventually form a dimer, a fraction of their hydration layers gradually disappears. Since the formation of a dimer requires total dehydration of the contacting surfaces of both sterols, the most crucial in the process is the behaviour of the layer *L1* water as it is the closest to the sterol molecule and relatively tightly bound to it. Two sterol molecules form a dimer when significant fragments of their surfaces are in contact i.e. when their Voronoi cells have common sides (are neighbours). The sum of the areas of the common sides defines the contact surface, which is given in the nm^2 units or as the % of the total molecular area. The contact surface of each molecule constitutes a fraction of its total surface, which, on the other hand, is the sum of the outer surfaces of the sterol's 3D Voronoi cells.

To describe the behaviour of water at the initiation of dimer formation, the concept of a water cross-layer is introduced. A cross-layer is formed when some of the water molecules in the hydration layers, e.g. *L1* of two sterol molecules, *M1* and *M2*, become common to both hydration layers. Using the Voronoi diagrams, it is possible to determine the number of these water molecules i.e. those belonging to the cross-layer *CL1*. The cross-layer *CL1* is the intersection of the layer *L1*(*M1*) with *L1*(*M2*). The appearance and growth of the cross-layer *CL1* and the decline of the hydration layers *L1*(*M1*) and *L1*(*M2*), and finally, the disappearance of the interfacial (between the contacting surfaces) fraction of the *CL1* water indicate the formation of a dimer.

2.4.2. Arrangement of sterol molecules in an aggregate

To establish the relative orientation of a pair of sterol molecules that form an aggregate a local orthogonal coordinate frame is assigned to each molecule. The frame (Fig. 5) is defined as follows, 1) its origin coincides with the position of the carbon atom C10 (Fig. 1); 2) its 'horizontal' plane is defined by three carbon atoms, C6, C10 and C13 (Fig. 1); 3) one of the two in-plane axes is defined by the line connecting C10 and C13 (**u**), the other is orthogonal to **u** and close to the line connecting C10 and C6 (**v**); 4) the third axis (**w**) is orthogonal to both **u** and **v**, and points in the direction indicated by the right-hand rule (Fig. 5) – the same as that of the methyl groups on the sterol rough side (Fig. 1).

The current relative orientation of two sterol molecules is defined by three angles formed between the two local coordinate frames (**u**, **v**, **w** and **u**′, **v**′, **w**′) of the molecules, i.e. **u-u**′, **v-v**′, **w-w**′ angles. Each angle can change within a range of 0° to 180° (0 and π radians, respectively). 0° means that two vectors are parallel to each other and point in the same direction; π means that the vectors are parallel and point in the opposite directions; 0.5π means that the vectors are perpendicular to each other. Both in the paper and SI, the **u** vector is red, the **v** is green and the **w** is blue, the plots of the corresponding angles in relevant figures are also given in the respective colours.

The distance between two sterol molecules forming a dimer is measured as interatomic separations between pairs of the corresponding C6, C10 and C13 atoms (cf. Fig. 1) of both molecules, that is by C6-C6, C10-C10 and C13-C13 distances. Plots of the distances in relevant figures are green, red and blue, respectively.

3. Results and discussion

3.1. Sterol-water interaction

3.1.1. Systems equilibration

The equilibration of the systems consisting of a sterol molecule inserted into the water box was observed during the initial 100 ps of MD simulation, sampled every 2 fs, whereas a very quick reaction of water on the appearance of the sterol monomer was observed during the first 2 ps of the MD simulation, sampled every 2 fs. This 'short-term' reaction and the details of the initial sterol hydration are described in detail and depicted in Fig. S3 in SI. Equilibration of the system was assessed by determining the time dependence of 1) the average distance between the sterol molecule

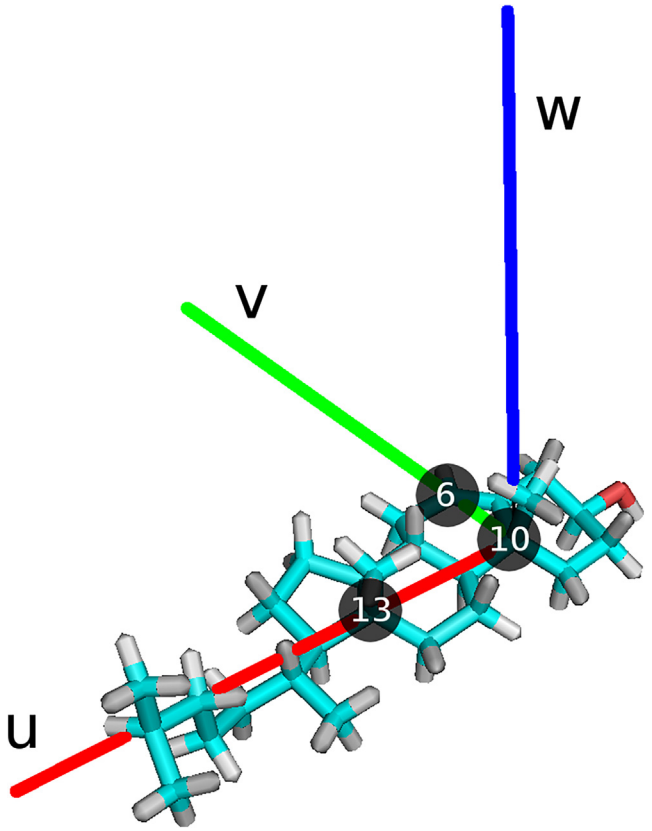

Fig. 5. Local orthogonal coordinate frame assigned to each sterol molecule. The carbon atoms C6, C10 and C16 (labelled) define the horizontal plane of the coordinate frame. The orthogonal axes of the coordinate frame are drawn in *red*, *green*, *blue* and labelled (see text). (For interpretation of the references to colour in this figure legend, the reader is referred to the web version of this article.)

and the water molecules from the first hydration shell (*L1*) as well as the average volume available to the sterol molecule, obtained from the Voronoi diagram analysis (Fig. 4); 2) the electrostatic and vdW energies of sterol-water and water-water interactions, obtained directly from unrestricted MD simulations.

The time profiles of the volume available to the Chol molecule (molecular volume) and the average *L1* water-Chol distance are shown in Fig. 6. Analogical plots for the other sterols are shown in Fig. S4 (SI). The time profiles of the Chol-water Coulomb and vdW energies are shown in Fig. 7 and those for the other sterols are shown in Fig. S5 (SI). The profiles in the figures demonstrate that during the first picoseconds of MD simulation all quantities visibly decrease and later on, they stabilised. The values of the molecular volume of sterol molecules and the average *L1* water-sterol distance are given in Table 1 and those of energies are given in Table 2. The values of the water-sterol distance and the vdW energy were similar for all sterols, whereas those of the sterol volume and the Coulomb energy depended on the number of polar groups on the sterol molecule (Table 2).

The initial decreases of all quantities had the same origin and were due to the formation of a water clathrate around the non-polar part of a sterol (Fig. 8) and sterol···water H-bonds (on average, ~ 2.4, ~ 4.3, and ~ 5.1 water molecules are H-bonded to the polar groups of Chol, 7-OH-Chol, and 7-OOH-Chol, respectively, cf. Section 3.1.2.1, Fig. 8). These sterol-water interactions imposed initial rearrangements of water molecules in the vicinity of the sterol molecule. The time scale of these initial water rearrangements (Figs. 6, 7, S4 and S5) was virtually the same as that of water molecule rotation in bulk water, of ~ 1.5–2.0 ps [57,58].

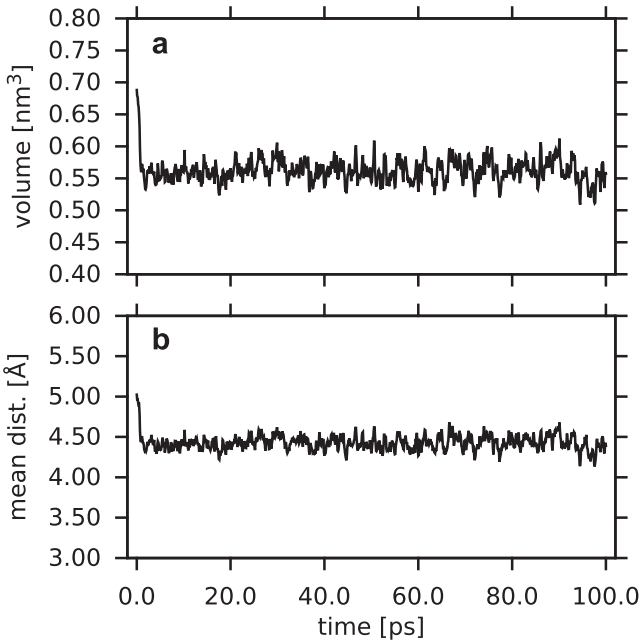

Fig. 6. Mean (a) volume available to the Chol molecule and (b) distance between Chol and the water molecules from *L1* as a function of time, during 100 ps, plotted every 100 fs.

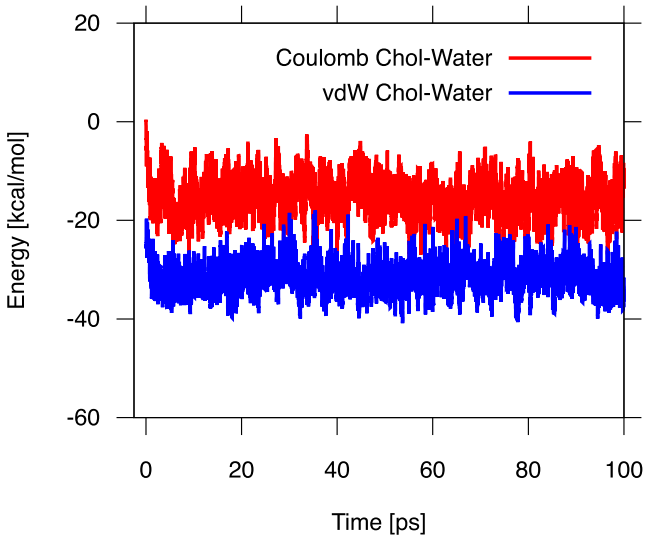

Fig. 7. Interaction energies of the pre-equilibrated Chol with water (Chol-water interaction), electrostatic (*red*); vdW (*blue*), during 100 ps, plotted every 2 fs. (For interpretation of the references to colour in this figure legend, the reader is referred to the web version of this article.)

The sterol-water interaction was attractive as both the Coulomb and vdW energies were negative (Figs. 7, S5). It is interesting to note that for the Chol-water interaction, the Coulomb energy is half of the vdW energy (Fig. 7) and for the sterols with an additional polar group the magnitude of both interactions is quite similar (Fig. S5).

The time profiles of the water-water Coulomb and vdW energies during the first 100 ps of MD simulation of a Chol monomer in water are shown in Fig. 9 a and b, respectively, and of oxChol monomers in Fig. S6 (SI). Evidently, bulk water-water interactions are affected neither by the Chol (Fig. 9) nor the oxChol (Fig. S6, SI) molecules. Figs. 9 and S6 additionally illustrate that the water-

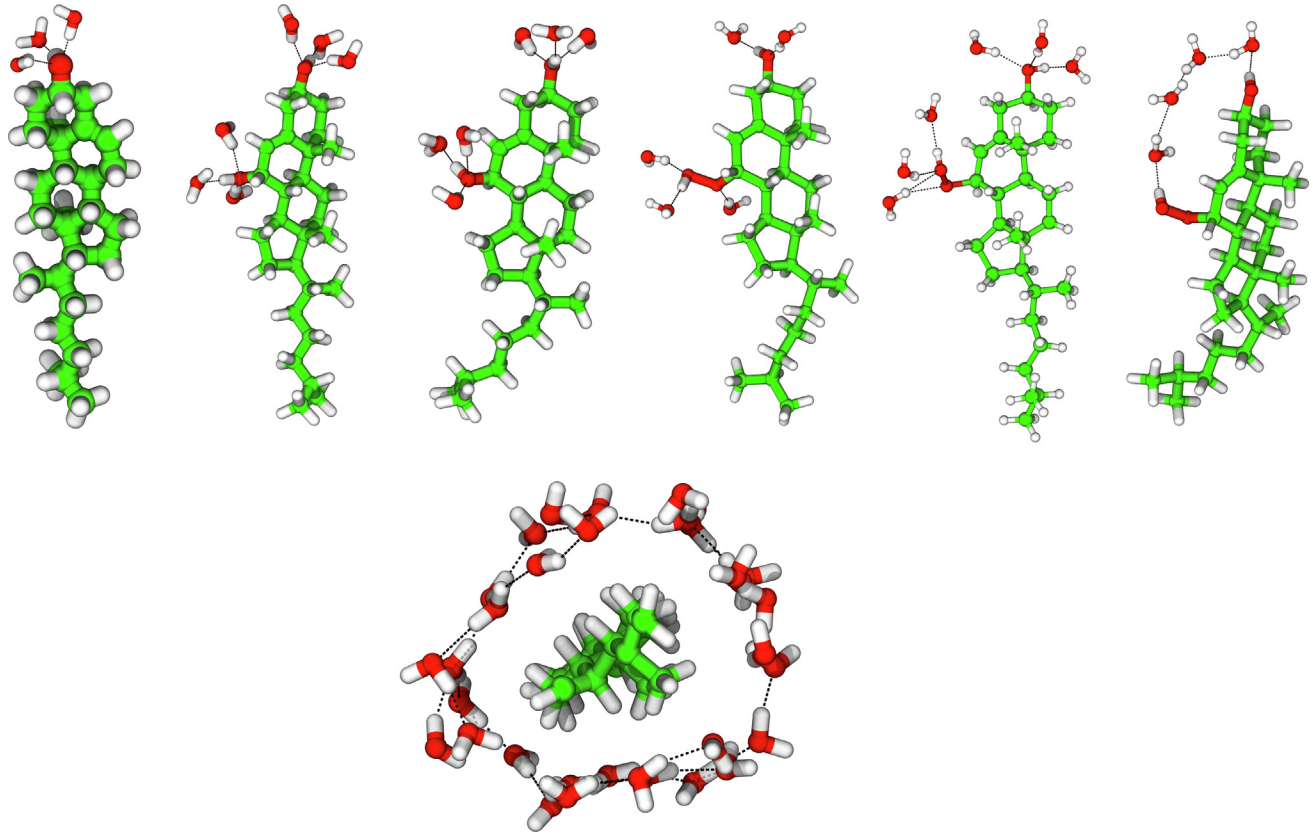

Fig. 8. Examples of direct interactions of water molecules with the sterol polar groups and the non-polar body. From left to right: water molecules H-bonded to Chol, 7α-OH-Chol, 7β-OH-Chol, 7α-OOH-Chol, 7β-OOH-Chol and linking the C3-OH and C7α-OOH groups of 7α-OOH-Chol; below: water clathrate around the Chol non-polar body.

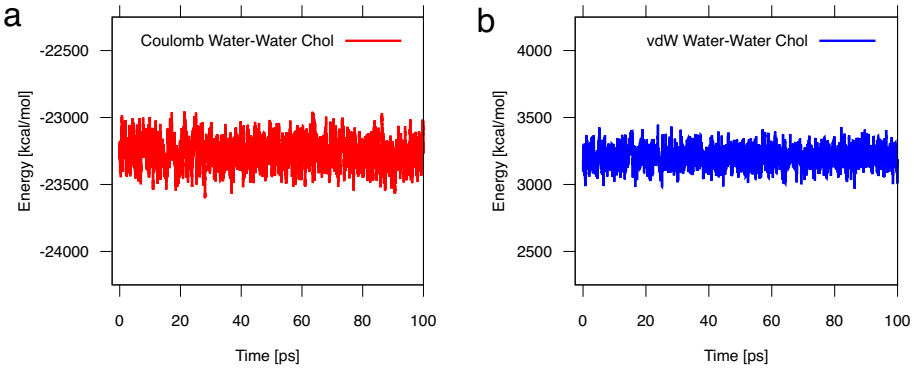

Fig. 9. Energies of water-water interactions, (a) Coulomb (*red*), (b) vdW (*blue*), during 100 ps, plotted every 2 fs. (For interpretation of the references to colour in this figure legend, the reader is referred to the web version of this article.)

water Coulomb interaction is attractive (negative), whereas the vdW interaction is repulsive (positive). The average internal (bonded) energy of a sterol molecule is stable from the beginning of MD simulation (no initial change of the energy), which implies that the initial decreases in the sterol-water distance and interaction energies were not caused by any structural changes of the sterol molecule and also that the internal energy does not depend on the volume available to the sterol molecule.

3.1.2. Equilibrated system

The results presented in Section 3.1.1 indicate that the water molecules belonging to *L1* react to the appearance of a sterol molecule. This reaction is short-term and lasts for less than 2 ps (Figs. 6, 7, S4 and S5), thus the system equilibrates quickly.

To study the properties at equilibrium, the systems consisting of a sterol molecule in a water box were MD simulated for 10 ns. Even though equilibration of the systems was fast, the first 1-ns fragment of the generated trajectories is not included in their analyses. The analyses concern 1) the organisation of water molecules interacting with the sterol monomer; 2) the exchange of water molecules H-bonded to the sterol OH and OOH groups (Fig. 8); 3) the exchange of water molecules clathrating the non-polar part of a sterol molecule (Fig. 8). In separate calculations 4) the hydration energy of each sterol molecule is obtained (cf. Section 2.3.1).

3.1.2.1. Water···sterol H-bonds. All sterol molecules studied in this paper have a hydroxyl group attached to the C3 carbon atom (C3-OH, Fig. 1). The oxChol molecules have an additional hydroxyl

or hydroperoxy group attached to the C7 carbon atom (C7-OH or C7-OOH, Figs. 2 and S1, SI). These polar groups are H-bond donors and acceptors. Water molecules are also donors and acceptors of H-bonds. Thus, the sterol polar groups make H-bonds with water readily through both oxygen and hydrogen atoms (Fig. 8). To identify H-bonded water molecules, the same criteria of the H-bond formation were used as in our previous paper [18]: H-bond distance of 3.5 Å and H-bond angle of 30° (when calculating the angle either the water or the Chol oxygen atom is the H-bond donor). For all sterols in water, the C3-OH group makes H-bonds with 2.3–2.4 water molecules similarly to the group of a Chol in the CBD [18]. 1.4–1.5 of them are H-bonded through the oxygen atom and ~ 0.9 through the hydrogen atom (Table 3). The C7-OH group binds fewer water molecules than C3-OH, ~ 2.0, and again more through the oxygen than the hydrogen atom (Table 3). In contrast, for the C7-OOH group the number of H-bonded water molecules through the hydrogen atom is almost the same as that through the hydroxyl (O) and the ether (O_{ET}) oxygen atoms (Table 3). Water molecules also form a chain linking both polar groups of oxChol, as illustrated in Fig. 8.

It is interesting to note that the volume of a water molecule in the first hydration layer (*L1*) of Chol of 31.52 ± 0.67 $Å^3$ is larger than in the second and third (*L2*, *L3*) of 30.0 ± 0.38 and 29.93 ± 0.26 $Å^3$, respectively, (Fig. S7). For other sterols, these values are very similar.

3.1.2.2. Ordering of water molecules by sterol. The ordering effect of the sterol hydroxy and hydroperoxy groups on water is evident in the radial distribution functions (RDFs) of water molecules relative to sterol polar groups shown in Fig. 10. RDFs of water molecules relative to the sterols' C3-OH group are compared in Fig. S8 (SI). This ordering of water results from water···sterol H-bonding (cf. Section 3.1.2.1).

The almost equal numbers of H-bonds between water and the O, O_{ET}, and H atoms of the C7-OOH group is not apparent from the RDFs in Fig. 10c. Due to the close distance between these atoms, RDFs of water relative to O and O_{ET}, 'see' water molecules ordered by both oxygen atoms and possibly also by the H atom. This results in distorted shapes and a broadening of the RDFs and shifting of their maxima. Thus, only a direct calculation of the number of H-bonded water molecules, based on geometric criteria, gives their proper number.

The non-polar body of a sterol molecule also has an ordering effect on the nearby water molecules that form a clathrate around it (Fig. 8). The water molecules in a clathrate are at a defined distance from the sterol molecule (cf. Table 1) and their mutual H-bonds are orientated tangent to the sterol surface (Fig. 8). This ordering effect can be seen as the maxima of the RFDs in Fig. 11. The Chol methyl groups (Chol-CH_3) located on the rough side of the sterol molecule (C18 and C19 in Fig. 1) have a relatively large ordering effect on water (Fig. 11c). A similar ordering was imposed by C18 and C19 on carbon atoms of the phosphatidylcholine (PC) acyl chains in the dimyristoyl-PC (DMPC) bilayer containing 22 mol% Chol [59].

3.1.2.3. Exchange of the sterol-bound water molecules with bulk. Water molecules that are H-bonded and clathrate a sterol molecule form together the sterol's *L1* water (cf. Section 2.4.1.1). The number of water molecules in *L1* is ~ 80, of which between 2.4 and 5, depending on the number and kind of the sterol's polar groups, are H-bonded (Table 3). These water molecules exchange with bulk water. Here, the characteristic exchange times of three groups of sterol-bound water molecules, i.e., forming a clathrate, H-bonded and belonging to *L1*, are assessed. A detailed description of the analysis of the exchange of the sterol-bound water molecules with bulk is given in SI. The decay curves illustrating the exchange processes of the Chol-bound water from the three groups together with the fitted curves are shown in Fig. 12 and of the oxChol-bound water in Fig. S9 (SI). The figures also indicate that the exchange is completed in less than 40 ps.

The goodness of fit (details are given in SI) is assessed by calculating the reduced χ^2 which in all cases is practically 1.0 and indicates a perfect fit of each decay curve to a sum of two exponential functions (Figs. 12 and S9, SI). Thus, each exchange process has two components, one is "slow" and the other is "fast". Each component has a characteristic exchange time (time constant), Tc, and the 'amplitude', A, indicating the contribution of the component in the decay process. The fitted parameters (Tc_i and A_i) are given in Table 4.

For all sterols, in the exchange process of the *L1* and clathrating water, the "slow" component with Tc between 7 and 8 ps makes a large contribution, of ~ 80%. A smaller contribution, of ~ 20%, is made by the "fast" component with Tc of 0.8–1.8 ps (Table 4). In the case of water H-bonded to C3-OH, Tc's of both components do not depend on the chemical structure of the sterol molecule (Table 4). Conversely, in the case of C7-OH of oxChol the rate of the H-bonded water exchange depends on the chirality of the group, and for the α form it is slower than for the β form (Table 4). The exchange is also slower for the C7-OOH α form than for the β form (Table 4). The contributions of the "slow" and "fast" components to the exchange processes of the water H-bonded to the sterols' polar groups are ~ 50–60% and ~ 40–50%, respectively (Table 4).

The contribution of components with different time constants to the exchange process of the water H-bonded to a PC head group was broadly discussed in Ref. [60]. That discussion is also relevant to water···sterol H-bonds analysed in this paper.

The exchange time of clathrating water is virtually the same for all sterols. This is because the clathrate is a network of mutually H-bonded water molecules, surrounding a sterol molecule, which are held at a specific distance from the sterol by the attractive vdW interactions. The exchange of these water molecules with bulk is relatively slow.

The differences between Tc's of water H-bonded to the C7-OH and C7-OOH groups for the α and the β form of oxChol possibly stem from the difference in the orientation of the groups in both forms and the likelihood that the water molecules H-bonded to these groups simultaneously participate in the water clathrate. The C7α-OH and C7α-OOH groups are oriented towards the oxChol smooth face (α-face, Fig. 1). The water molecules H-bonded to these groups belong to the firm clathrate structure, and even though the polar groups might somewhat disturb it, their exchange time with bulk is similar to that of the clathrating water. The C7β-OH and C7β-OOH groups are oriented towards the rough face (β-face, Fig. 1) of the steroid moiety. On this side, the clathrate is perturbed by the two CH_3 groups and the polar groups might additionally destabilise it. In effect, the network of the clathrating water is looser and possibly has a smaller effect on the water molecules H-bonded to C7β-OH and C7β-OOH. Thus, they exchange with bulk similarly quickly as those H-bonded to C3-OH, which only weakly participate in the clathrating water network.

3.1.2.4. Energy of sterol hydration. As stated in the Methods section, the energy of hydration is the Gibbs free energy change (ΔG) when a solute molecule is transferred from vacuum to water. This energy is calculated using the FEP method (cf. Section 2.3.1). The values of the energy for the sterols studied here are given in Table 5.

The negative values of the energy of hydration for all sterols (Table 5) indicate that the transfer of each sterol molecule from vacuum to water is energetically favourable even though the entropy of the system decreases due to reduction in the water mobility, particularly that from the first and second hydration shells (Fig. S7, SI). The transfer is energetically favourable because

Table 3
Number of water molecules H-bonded to the polar groups of a sterol monomer in water.

Sterol/Polar group	Chol	O7a	O7b	OO7a	OO7b
OH-C3	2.38 ± 0.71	2.32 ± 0.70	2.32 ± 0.74	2.32 ± 0.72	2.33 ± 0.73
OH-C3	1.50 ± 0.60	1.44 ± 0.60	1.47 ± 0.60	1.44 ± 0.59	1.47 ± 0.61
O**H**-C3	0.88 ± 0.34	0.88 ± 0.34	0.85 ± 0.37	0.88 ± 0.34	0.86 ± 0.37
OH-C7/OOH-C7		1.98 ± 0.80	2.02 ± 0.76	2.85 ± 0.83	2.67 ± 0.79
OH-C7		1.28 ± 0.60	1.28 ± 0.59	1.06 ± 0.67	0.95 ± 0.65
O**H**-C7		0.70 ± 0.46	0.74 ± 0.44	0.88 ± 0.35	0.83 ± 0.39
O$_{ET}$-C7				0.91 ± 0.64	0.89 ± 0.65
Total	2.38 ± 0.71	4.30 ± 1.1	4.34 ± 1.1	5.17 ± 1.1	5.0 ± 1.1

The average numbers of H-bonded water molecules to OH and OOH groups attached to the C3 and C7 atoms of the monomeric sterol molecules and separately to the hydroxy and ether oxygen (**O**H-C3, **O**H-C7, **O**$_{ET}$-C7) and hydrogen (O**H**-C3, O**H**-C7) atoms (the bonding atom is marked bold) of Chol; 7α-OH-Chol (O7a); 7β-OH-Chol (O7b); 7α-OOH-Chol (OO7a); 7β-OOH-Chol (OO7b) in water, for systems in equilibrium. The total number of H-bonded water molecules per sterol molecule is given in the bottom row. Errors are standard deviations relative to time averages over 1 ns time periods.

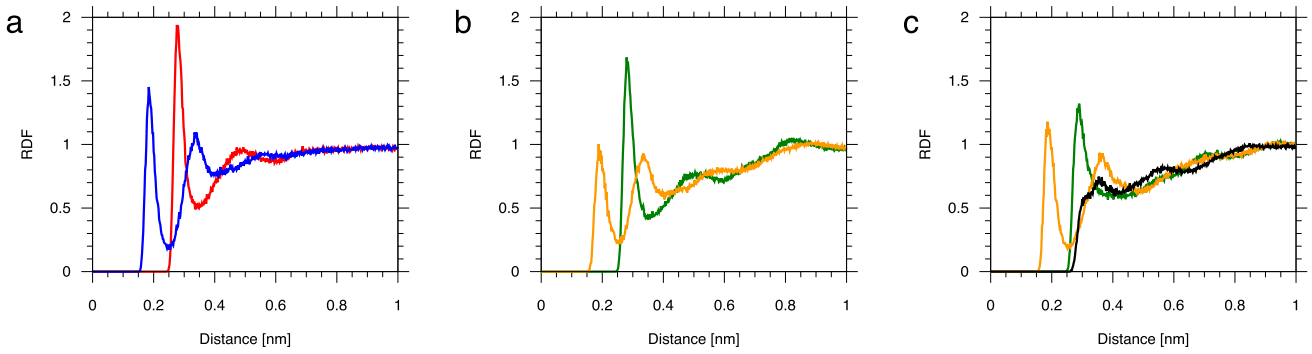

Fig. 10. Radial distribution functions (RDF) of water oxygen atoms relative to a sterol (a) C3-OH; (b) C7-OH; (c) C7-OOH group. (a) C3-OH O atom (*red*), C3-OH H atom (*blue*); (b) C7-OH O atom (*green*), C7-OH H atom (*yellow*); (c) C7-OOH hydroxyl O atom (*green*), ether O$_{ET}$ atom (*black*) and hydroxyl H atom (*yellow*). (For interpretation of the references to colour in this figure legend, the reader is referred to the web version of this article.)

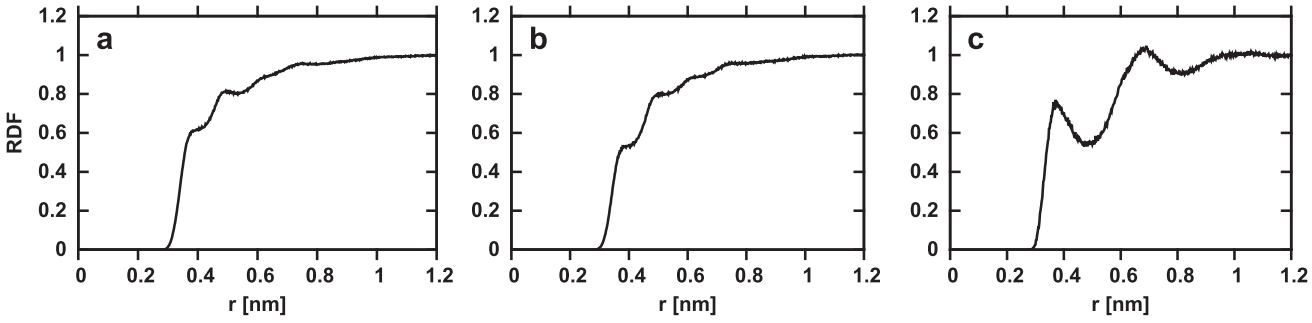

Fig. 11. RDFs of water oxygen atoms relative to (a) all Chol C atoms; (b) C atoms of the Chol ring; (c) Chol methyl groups (Chol-CH$_3$) located on the rough side of the sterol molecule (C18 and C19 in Fig. 1).

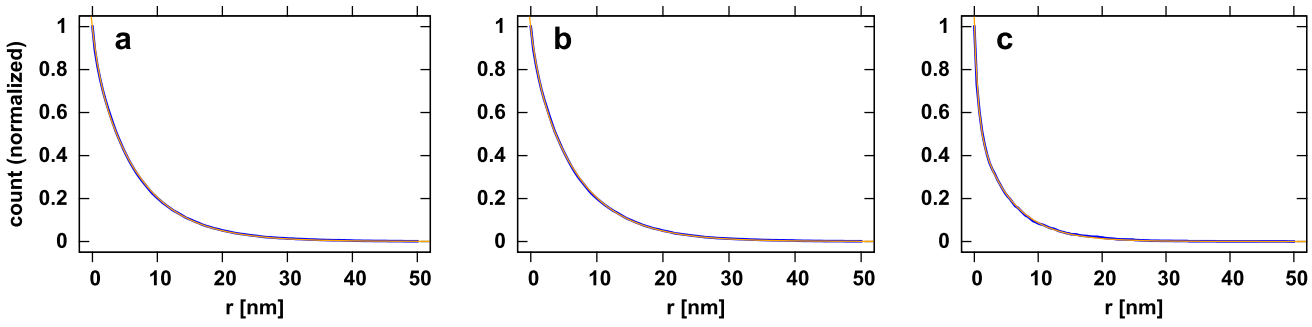

Fig. 12. Exchange of the Chol-bound water with bulk. (a) *L1*, (b) clathrating, and (c) H-bonded water. The decay curve (*blue*) of the initial number of water molecules in a given group is fitted to two exponential functions (*orange*); the *blue* and *orange* curves are superimposed and overlap with each other. The reduced χ^2 of all fits is essentially 1.0, which indicates perfect fits. (For interpretation of the references to colour in this figure legend, the reader is referred to the web version of this article.)

Table 4
Exchange of sterol-bound water molecules with bulk.

Sterol	Water group	A_1 [%]	Tc_1 [ps]	A_2 [%]	Tc_2 [ps]
Chol	L1	83.8 ± 0.3	7.08 ± 0.02	15.5 ± 0.4	0.96 ± 0.03
	Clathrate	84.6 ± 0.4	7.02 ± 0.02	14.6 ± 0.4	1.11 ± 0.05
	OH-C3	56.0 ± 0.3	5.38 ± 0.03	43.6 ± 0.4	0.60 ± 0.01
O7a	L1	76.9 ± 0.8	7.89 ± 0.05	21.4 ± 0.7	1.83 ± 0.08
	Clathrate	82.4 ± 0.6	7.32 ± 0.04	16.3 ± 0.6	1.49 ± 0.08
	OH-C3	54.0 ± 0.3	5.78 ± 0.03	45.5 ± 0.4	0.70 ± 0.01
	OH-C7	59.5 ± 0.4	7.32 ± 0.05	39.4 ± 0.5	0.71 ± 0.02
O7b	L1	82.1 ± 0.4	7.58 ± 0.03	16.9 ± 0.4	1.13 ± 0.05
	Clathrate	84.4 ± 0.4	7.27 ± 0.03	14.8 ± 0.3	1.03 ± 0.05
	OH-C3	56.8 ± 0.4	5.56 ± 0.04	42.5 ± 0.5	0.66 ± 0.02
	OH-C7	63.8 ± 0.3	5.72 ± 0.02	35.8 ± 0.3	0.63 ± 0.01
OO7a	L1	78.3 ± 0.7	7.64 ± 0.05	20.2 ± 0.7	1.41 ± 0.07
	Clathrate	82.9 ± 0.5	7.07 ± 0.03	16.1 ± 0.5	1.16 ± 0.06
	OH-C3	59.3 ± 0.4	5.16 ± 0.03	40.1 ± 0.4	0.61 ± 0.01
	OOH-C7	48.0 ± 1.1	6.92 ± 0.12	50.0 ± 1.1	1.27 ± 0.05
OO7b	L1	79.9 ± 0.4	7.43 ± 0.03	19.1 ± 0.4	1.28 ± 0.05
	Clathrate	83.2 ± 0.4	6.90 ± 0.03	15.8 ± 0.4	1.16 ± 0.05
	OH-C3	57.7 ± 0.2	5.15 ± 0.02	41.9 ± 0.3	0.63 ± 0.08
	OOH-C7	58.1 ± 0.5	5.35 ± 0.04	41.0 ± 0.5	0.86 ± 0.02

Parameters of two-exponential non-linear fits to decay curves of the number of water molecules in the first hydration layer (*L1*); clathrating water (Clathrate); water H-bonded to the OH-C3, OH-C7 and OOH-C7 polar groups, of the sterol molecule. Contribution (A_i, %) and time constant (Tc_i, ps) of the individual decay curves for Chol (Chol); 7α-OH-Chol (O7a); 7β-OH-Chol (O7b); 7α-OOH-Chol (OO7a); 7β-OOH-Chol (OO7b). Errors of the fitted parameters correspond to standard errors.

Table 5
The Gibbs free energy change (ΔG) when a sterol molecule is transferred from vacuum to water.

Sterol	ΔG [kcal/mol]
Chol	−4.70 ± 0.17
7α-OH-Chol	−8.94 ± 0.18
7β-OH-Chol	−9.68 ± 0.16
7α-OOH-Chol	−8.96 ± 0.13
7β-OOH-Chol	−8.32 ± 0.15

Abbreviations used in the Table are explained in the text (α and β are chiral forms of the hydroxy and hydroperoxy groups, '7' refers to the C7 carbon atom of the sterol molecule, cf. Fig. 1).

H-bonds that are formed between the sterol polar groups and water decease the system's Coulomb energy and also because, as Figs. 7 and S5 show, the vdW interactions between the sterol and water are attractive (negative) which further decreases the system's energy. As oxChols have additional polar groups able to make H-bonds with water, their transfer lowers the energy of the system more than that of a Chol molecule. At the same time, the Coulomb and vdW sterol-water interactions order water molecules in the vicinity of the sterol molecule, which restricts their motion and decreases entropy of the system. Thus, the energy gain on transferring Chol from a vacuum to water is similar to the energy of a single water···water H-bond of 4.4 – 5.5 kcal/mol [61,62]; for oxChol it is larger.

The values of the sterol-water nonbonded interactions (Table 2) as well as those of the free energy of sterol hydration (Table 5) can be compared to those obtained for tryptophan, whose chemical structure is somewhat similar to that of an oxChol molecule. The enthalpy of hydration for tryptophan is ~ −34 kcal/mol and the free energy is ~ −12 kcal/mol [63]. These values are within the range of those for oxChols of ~ −55 and ~ −9 kcal/mol, respectively, (Tables 2 and 5). For all amino acids, independent of their hydrophobicity, the energy of hydration is negative and decreases with the number of polar groups and net electrostatic charge. A similar trend is observed for Chol and oxChols.

3.2. Chol-sterol interaction in water

3.2.1. Chol-sterol dimer formation

The behaviour of two sterol molecules inserted into a water box was generated in 10-ns MD simulation. One of the sterol molecules was Chol and the other was either Chol or one of the four oxChol species. Even though the encounter of two mainly non-polar molecules in water is to a large extent a random event, in all systems, the two sterol molecules formed a dimer in much less than 10 ns (Figs. 13, S10 and S11).

The formation, integrity and geometrical stability of a dimer were assessed by monitoring the relative position of the molecules, determined by the C6-C6, C10-C10 and C13-C13 distances (cf. Fig. 1, Section 2.4.2); the relative orientation of the molecules, uniquely defined by three angles between the corresponding orthogonal vectors assigned to each molecule (Fig. 5, Section 2.4.2); the area of the common surface and the volumes of the sterols hydration layers, obtained from the Voronoi analysis (Section 2.4.1); and the Coulomb and vdW Chol-sterol interaction energies, obtained from group interaction energy calculations. These quantities as functions of time during 10 ns are shown in Figs. 13, 14, S10–S13 (SI). It should be noted, however, that the interatomic distances in the dimer that formed depended on which surfaces of the sterol molecules (smooth, rough) were in contact and whether the molecules were in the head-to-head or head-to-tail relative orientations (see below).

Time profiles of the three angles and distances, the common area, and the two energies for the Chol-Chol dimer are displayed in Fig. 13, and for the Chol-oxChol dimers in Figs. S10 and S11 (SI). The process of Chol-Chol dimer formation and the subsequent behaviour of the Chol molecules in the dimer during 10-ns MD simulation are shown in film SF1 (SI), as an example. The formation and the behaviour of Chol-oxChol dimers followed a similar course. The film SF1 and the figures reveal the dynamic character of the Chol-sterol dimers, which can be recognised in the figures as significant fluctuations in all measured quantities. Moreover, the three angles not only fluctuate but also drastically change their values. Changes of ~ 90° (½π) are rare and short-term; changes of ~ 180° (π) occur more often and last for a longer time. The latter changes imply that one molecule reverses its orientation relative to the other. Yet the profiles indicate that irrespective of these reori-

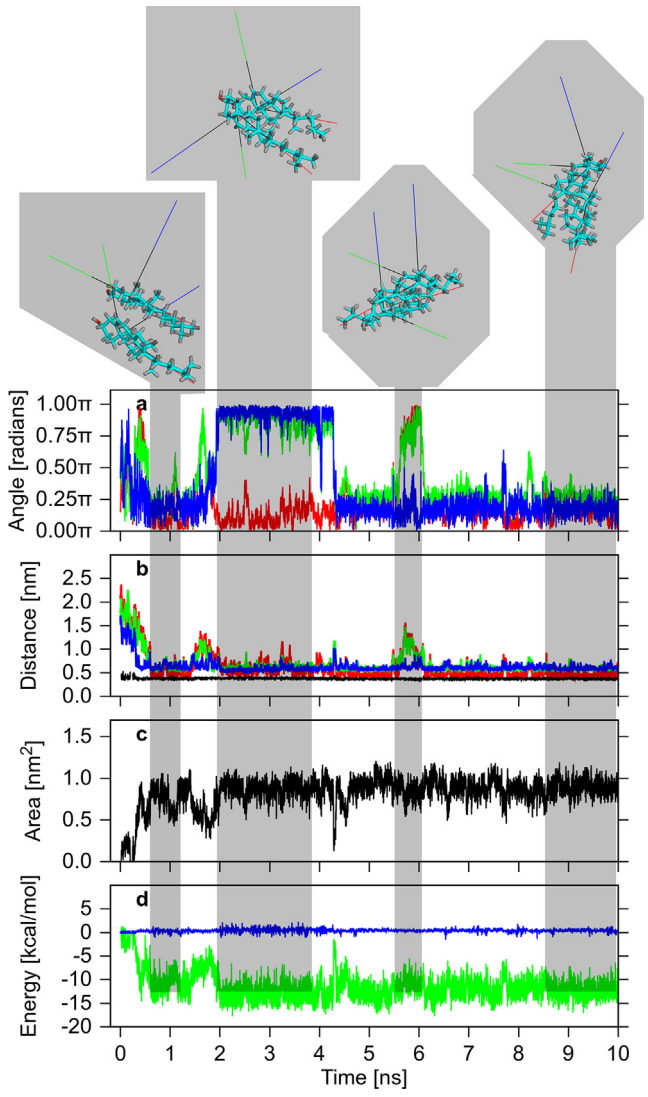

Fig. 13. Time courses of the relative orientation, distance, contact area and intermolecular interaction energies of two Chol molecules in water before and after dimer formation, together with snapshots of the representative configurations of the molecules in the dimer. The *grey* areas connect configurations of the molecules in the dimer (at the top) with the numerical values of (a) angles between corresponding vectors, **u** (*red*), **v** (*green*) and **w** (*blue*); (b) distances between the C6 (*red*), C10 (*green*) and C13 (*blue*) atoms (cf. Section 2.4.2) and the smallest distance between any atoms (*black*), of both molecules; (c) area of the contact surface; (d) energies of Coulomb (*blue*) and vdW (*green*) Chol-Chol interactions. Noise in the time profiles indicates the dynamic nature of the relatively stable dimer, whereas temporary simultaneous changes of ~ 180° (π) in any two angles illustrate that one molecule reverses its orientation relative to the other. (For interpretation of the references to colour in this figure legend, the reader is referred to the web version of this article.)

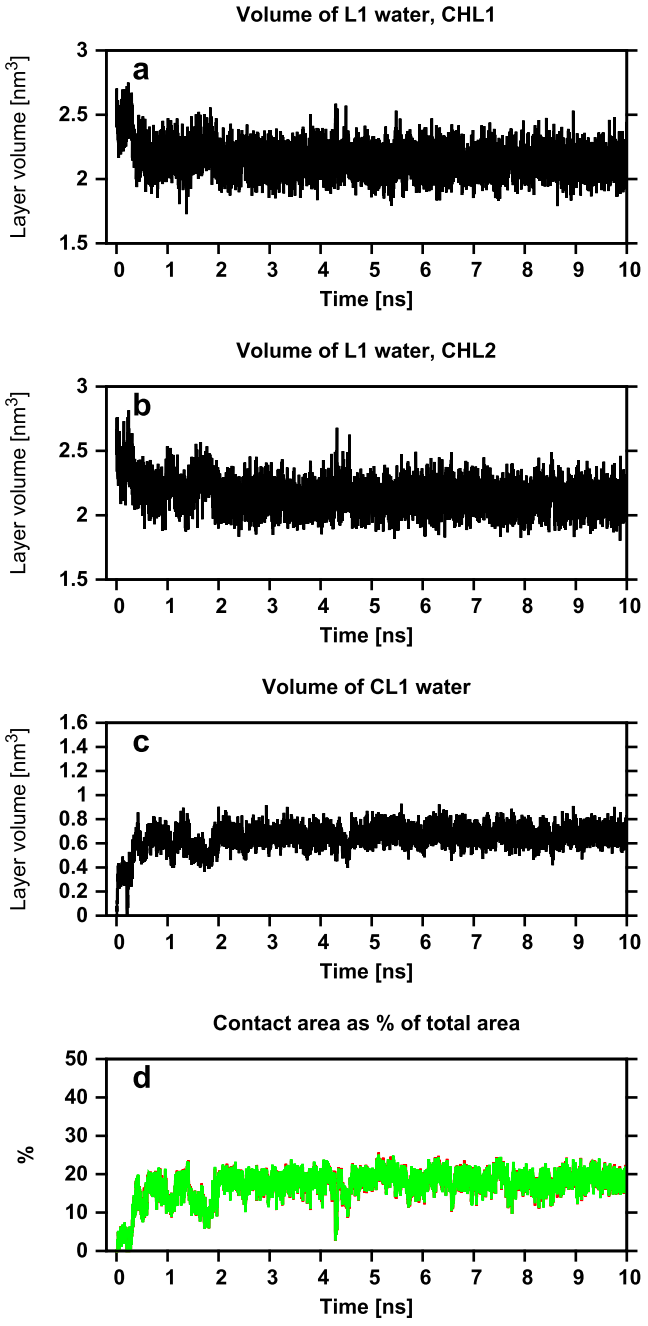

Fig. 14. Dehydration of contacting surfaces of two Chol molecules during dimer formation. Time profiles of the volume of the layer *L1* water of (a) Chol1 (CHL1) and (b) Chol2 (CHL2) forming a Chol-Chol dimer, (c) the cross-layer *CL1* water of both molecules and (d) area of the contact surface as % of the total area of each sterol molecule – the *red* (Chol1) and *green* (Chol2) lines overlap. (For interpretation of the references to colour in this figure legend, the reader is referred to the web version of this article.)

entations and fluctuations, once the dimer is formed the molecules remain in contact and the dimer preserves its integrity.

Figs. 13, 14, S10-S13 (SI) illustrate the initial processes that take place when two sterol molecules are inserted in water. The figures indicate that during the first 10 ns, not only a dimer is formed but it also often undergoes geometrical rearrangements. A detailed inspection of the time profiles in Fig. 13 indicates that the configuration of the initially formed Chol-Chol dimer is smooth-rough, where the smooth surface (α-face, Fig. 1) of one molecule faces the rough surface (β-face, Fig. 1) of the other, and head-to-head, where the C3-OH groups of both molecules are on the same side of the dimer (Fig. S14, row #1). However, this configuration is not stable. Then the dimer's configuration converts to the smooth-smooth for ~ 2.5 ns. In this state, the vdW energy is low and stable but the Coulomb energy makes a relatively large positive contribution and together with the distances and angles, fluctuates significantly, which destabilises the dimer (Fig. 13; Table 6). At ~ 4.5 ns, the dimer returns to the smooth-rough configuration where the vdW energy has a higher value than for the previous one and fluctuates more. Nonetheless, the distances, angles, Coulomb energy and contact area fluctuate less (Table 6) except for some instability at ~ 5.5 ns, when the configuration of the

Table 6
Relative orientation and distance between sterol molecules in the dimer.

Dimer	Time [ns]	**u-u′** [°]	**v-v′** [°]	**w-w′** [°]	C6-C6 [Å]	C10-C10 [Å]	C13-C13 [Å]	E_{vdW} [kcal/mol]	E_{Coul} [kcal/mol]
Chol-Chol	2.5 - 4.0	24.4 ± 14.7	153.2 ± 14.5	166.4 ± 8.9	5.9 ± 1.4	6.2 ± 0.6	5.8 ± 0.4	-12.9 ± 1.6	0.5 ± 0.3
	4.5 - 5.5	38.1 ± 15.7	50.0 ± 12.2	30.6 ± 9.0	4.8 ± 1.0	5.8 ± 0.4	5.9 ± 0.4	-12.5 ± 1.9	0.4 ± 0.2
	6.5 - 10.0	30.8 ± 17.0	47.4 ± 14.5	33.7 ± 11.8	4.8 ± 0.8	5.9 ± 0.5	6.1 ± 0.4	-12.1 ± 1.7	0.4 ± 0.2
Chol–O7a	4.0 - 6.0	148.3 ± 11.8	148.5 ± 14.1	21.2 ± 11.0	6.5 ± 0.8	7.3 ± 0.4	7.3 ± 0.6	-11.9 ± 1.2	0.3 ± 0.2
	8.0 - 10.0	36.7 ± 11.0	48.6 ± 9.5	30.8 ± 6.8	4.6 ± 0.5	5.7 ± 0.4	5.7 ± 0.2	-13.7 ± 1.2	0.4 ± 0.2
Chol–O7b	3.5 - 9.0	17.0 ± 11.1	40.6 ± 10.1	35.8 ± 8.6	4.5 ± 0.5	5.8 ± 0.3	5.9 ± 0.4	-12.3 ± 1.5	0.3 ± 0.3
	9.0 - 10.0	156.3 ± 12.7	153.9 ± 10.6	14.9 ± 6.9	7.7 ± 0.9	8.0 ± 0.6	6.6 ± 0.4	-11.1 ± 2.0	0.3 ± 0.2
Chol–OO7a	2.0 - 5.0	13.1 ± 11.9	24.1 ± 10.2	20.1 ± 8.3	5.2 ± 0.5	5.9 ± 0.3	6.0 ± 0.3	-12.7 ± 1.5	0.03 ± 0.3
Chol–OO7b	3.0 - 10.0	154.6 ± 12.4	38.2 ± 9.8	153.8 ± 9.2	9.6 ± 1.8	9.5 ± 1.6	5.7 ± 0.5	-14.3 ± 1.5	0.4 ± 0.2

Average values of the **u-u′**, **v-v′**, **w-w′** angles, C6-C6, C10-C10, C13-C13 distances (defined in Section 2.4.2) and the energy of sterol-sterol vdW (E_{vdW}) and Coulomb (E_{Coul}) interactions for time periods when the dimer is in a stable state (Time); the grey areas indicate the seemingly optimal smooth-rough, head-to-head configurations of the molecules in the dimers and also stable smooth-smooth, head-to-tail configuration of the Chol–OO7b dimer; the names of the dimers are abbreviated, cf. the main text.

molecules changes temporarily to head-to-tail and then returns to the previous one. The instabilities in the dimer structure are associated with the reversal of the relative orientation of the molecules in the dimer (Fig. 13).

It is somewhat puzzling why the configuration of the molecules in the Chol-Chol dimer in water is not mainly smooth-smooth. At this configuration the Chol rings are almost parallel to each other (Fig. S14, row #1), the vertical distance between the rings is less than 4.5 Å and their vdW interactions are strong, which a relevant fragment of the energy profile in Fig. 13 indicates. The smooth-smooth configuration of the Chol dimer is the preferred one in lipid bilayers [64–66]. However, this geometry of the dimer in water probably causes unnecessary additional ordering of water molecules by the Chol-CH_3 groups exposed to water of both Chol molecules (Figs. 1, S14, row #1). The groups, as evidenced in Fig. 11c, have a relatively strong ordering effect on the neighbouring water molecules. In the smooth-rough configuration, only the rough face of one Chol is exposed to water; in effect the neighbouring water is less ordered and water entropy less decreased.

To assess better the integrity and geometrical stability of the Chol-Chol dimer in water, the 10-ns MD simulation was extended to 100 ns. The time courses of the relative orientation, distance, contact area and intermolecular interaction energies of two Chol molecules over 100 ns are shown in Fig. S10 (SI). The profiles clearly show that once the dimer is formed it preserves its integrity even though the relative configuration of the molecules in the dimer is changing constantly and does not tend to a definite one. In fact, Figs. S10 and S12 (SI) indicate that at ~ 42nd ns of MD simulation the Chol-Chol dimer disintegrates for a short while, nevertheless, it integrates again to remain in that state for the next ~ 55 ns of MD simulation. The longer MD simulation reveals that, in addition to the smooth-rough and smooth-smooth head-to-head configurations, a smooth-smooth head-to-tail is also quite populated. Such a configuration is rather unlikely in the lipid bilayer because it introduces a polar group in the bilayer centre. The 100-ns MD simulation is certainly preferred to show the dynamic character of the dimer in water (Fig. S10, SI), although the 10-ns MD simulation is better for showing the initial processes that lead to dimer formation such as dehydration of the interfacial surfaces of the sterol molecules, formation of the cross-layer and the contact surface (Fig. 14) as well as the time scales of these processes. Besides, based on the 10-ns MD simulation results the general conclusion can already be drawn that the Chol-Chol and also Chol-oxChol dimers are dynamic entities (film SF1, SI).

In the Chol-oxChols dimers, the additional polar groups at C7 strongly interact with water (Figs. 8 and 10, Table 3), so it is rather unlikely that they are placed between the rings of the sterols in the dimer. Thus, for the α form, oxChol is expected to be turned towards Chol with its rough face and for the β form, with its smooth face.

A relatively stable Chol–O7a (abbr. from Chol–7α-OH-Chol) dimer with smooth-rough, head-to-head configuration (Figs. 15 and S14, row #2), limited fluctuations and low values of interatomic distances, of ~ 0.5 nm, and vdW energy, of 13.7 kcal/mol (Table 6) is formed only after ~ 7 ns (Fig. S10). Here, as expected, the oxChol opposes Chol with its rough face (Fig. 15). For the previous several nanoseconds, the configuration is head-to-tail where the C6, C10 and C13 atoms of one molecule are in the reversed positions relative to those in the other. As a result, the C6-C6, C10-C10 and C13-C13 distances are > 0.5 nm, nevertheless they are quite stable (Table 6, Fig. S10). Nevertheless, the time profiles of the contact area and the vdW energy shown in Fig. S10 (SI), clearly indicate that the smooth-rough dimer in the head-to-head configuration is more stable than in the head-to-tail one (Table 6, Fig. S10).

The unexpectedly stable smooth-rough, head-to-head configuration of the Chol–OO7a (abbr. from Chol–7α-OOH-Chol) dimer is achieved within ~ 2 ns and remains such during the whole MD simulation, except for a short instability at ~ 7 ns (Fig. S11, SI). Against earlier anticipation, here the oxChol opposes Chol with its smooth face (Figs. 15, S14, row #4). Thus, the polar OOH group is located between the rings. But a closer look at the molecules in Fig. S14 row #4 (SI) demonstrates that the Chol ring is shifted parallelly relative to the oxChol ring, in effect the OOH group is well outside the contact surface and its interference with the non-polar intermolecular interactions is minimised. The values for the three angles in Table 6 indicate that the rings of both molecules

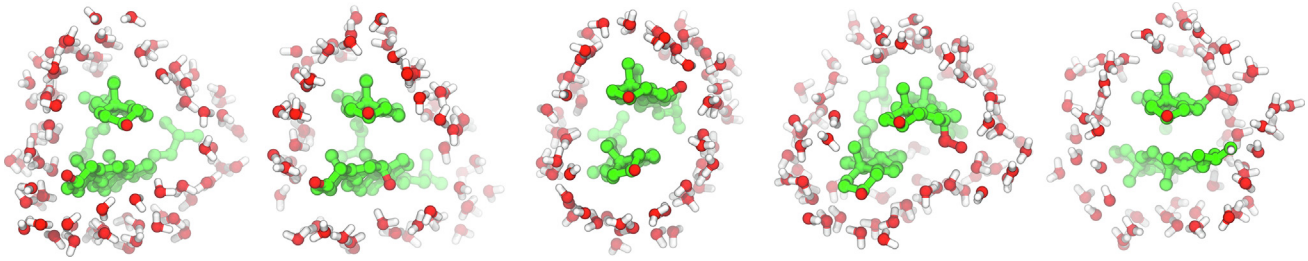

Fig. 15. Relative orientations of sterol molecules in the dimers and distribution of the water molecules form *L1* of each sterol. From left to right: the smooth-rough head-to-head configuration of the Chol-Chol; Chol–O7a; Chol–O7b; Chol–OO7a dimers, and the smooth-smooth head-to-tail configuration of the Chol–OO7b dimer.

are indeed almost parallel to each other. The packing of the molecules in the dimer is best illustrated in the CPK model in Fig. S14 (row #4, right).

The Chol–O7b (abbr. from Chol–7β-OH-Chol) dimer adopts a quite stable smooth-rough, head-to-head configuration within less than 3.5 ns (Fig. S10, SI). Here, the Chol opposes oxChol with its rough face (Figs. 15, S14, row #3). Stability of this configuration can be rationalised using the same arguments as in the case of the Chol-Chol dimer. Nevertheless, during the last ns of MD simulation one of the molecules rotates ~ 180° relative to the other and the dimer adopts the head-to-tail configuration, which increases the C6-C6, C10-C10 and C13-C13 distances, destabilises the vdW energy and decreases the intermolecular contact area (Table 6, Fig. S10).

The Chol–OO7b (abbr. from Chol–7β-OOH-Chol) dimer forms within ~ 2 ns of MD simulation in a somehow expected stable, smooth-smooth head-to-tail geometry (Fig. S11, SI). This means that against unfavourable entropic contribution, Chol and oxChol expose their CH_3 groups to the water phase (Figs. 15, S14, row #5). But the smooth-smooth geometry results in a strong intermolecular vdW attraction (Table 6), which, most likely, counterbalances decreased entropy.

The rough-rough configuration of the sterol molecules in a dimer formed in water is energetically and sterically unfavourable and it never occurred in these MD simulations, although it was observed in lipid bilayers [65,66].

Despite poor statistics, on the basis of the results presented in Figs. 13, S10 and S11 one can conclude that in the 10-ns MD simulation, except for the Chol–7β-OOH-Chol dimer, the smooth-rough head-to-head arrangement of molecules in the Chol-sterol dimers is the most prevalent or firm. In smooth-rough Chol-Chol and Chol–7α,β-OH-Chol dimers, the C6-C6 distances, of 4.5–4.8 Å, are smaller than the C10-C10 and C13-C13 distances, of 5.7–6.0 Å (Table 6). This is because the rings of the sterol molecules are angled relative to each other along the edge defined by the C6, C7, C15 carbon atoms (Fig. 15), with the average **v-v′** and **w-w′** angles (*green* and *blue*, respectively, in Figs. 13, S10 and S11) within a range of 40 to 50° and 30 to 35°, respectively, (Table 6). This tilting is necessary to enable better accommodation of the C18 and C19 methyl groups between the contacting surfaces. However, in the smooth-rough Chol-OO7a dimer, where the steroid rings are almost parallel to each other, the accommodation of the Chol C18 and C19 methyl groups and the "isolation" of the polar OOH group are facilitated by the relative shift of the rings along the **v**-axis (Figs. 5, 15, and S14, row #4). At the head-to-head configuration the contact area of the molecules is larger than otherwise—this is particularly apparent in the case of the Chol–O7a dimer (Fig. S10), but also of the Chol-Chol and Chol–O7b dimers (Figs. 13 and S10). This orientation enables water-mediated H-bonds to form between the C3-OH groups, as well as the C3-OH and C7-OH or C7-OOH groups of both sterol molecules in the dimer (Fig. 16), which additionally stabilises its structure. However, as Figs. 13, S10 and S11 and particularly Fig. S10 for the Chol-Chol dimer MD simulated for 100 ns clearly demonstrate, the molecules' positions and orientations in the dimers fluctuate significantly and reorientations are common, thus the dimers are dynamic.

3.2.2. Dehydration of contacting surfaces on dimer formation

An interesting and important aspect of Chol-sterol aggregation in water is the total dehydration of the contacting (interfacial) surfaces of the sterol molecules just before the dimer is formed (cf. Section 2.4.1.2).

The process of dehydration is monitored, using the Voronoi analysis, by recording the growth in the volume of the cross-layer *CL1* water with the concomitant decrease in the volumes of the *L1* water (cf. Section 2.4.1.2) of both molecules (Figs. 14, S12 and S13). As the time profiles in Figs. 14, S12 and S13 indicate, once the dimer is formed, the volumes of the *L1* water of each molecule and the *CL1* water stabilise. This is because the *L1* and *CL1* water disappears only from the surfaces that are in contact; the *L1* water still covers the non-contacting surfaces of the molecules, whereas the *CL1* water forms a ring-like structure surrounding the dimer in its horizontal plane. The distributions of the *L1* and *CL1* water around the Chol-Chol dimer are shown in Fig. 17 and the total dehydration of the contacting surfaces in all dimers is evident in Fig. 15.

The subsequent steps of the dehydration process can be seen in film SF2 (SI) as the growth of the interfacial fraction of cross-layer *CL1* water due to the merging of the interfacial fractions of the *L1* water of two Chol molecules approaching each other (cf. Section 2.4.1.2), and the final disappearance of the interfacial fraction of *CL1* on the Chol-Chol dimer formation. The rehydration and dehydration of the contacting surfaces during the reorganisation of the molecules in the Chol-Chol dimer can also be seen.

It is also interesting to compare the number of water molecules H-bonded to each sterol molecule in the monomeric (Table 3) and dimeric (Table S1, SI) states in water. The numbers for dimers are practically the same as for monomers, which proves that the polar groups of the sterols in the dimer are well exposed to water.

3.2.3. Free energy of dimer formation

The free energy of the association of two sterol molecules in water is calculated using the US method (cf. Section 2.3.2). The free energy profiles along the reaction coordinates (potential of mean force, PMF) obtained from US simulations are shown in Fig. 18. The profiles are shifted to a value of 0 kcal/mol for the monomeric states and corrected by the addition of the volume correction factor $2kT\ln(4\pi r^2)$ [67]. From each profile, the average free energy change is obtained as the difference between the minimum (dimeric state) and the initial (monomeric state) energy values. The values of the free energy change on sterols dimerisation are given in Table 7.

The negative values of the Gibbs free energy change (ΔG) indicate that the Chol-sterol association in water is spontaneous, thus

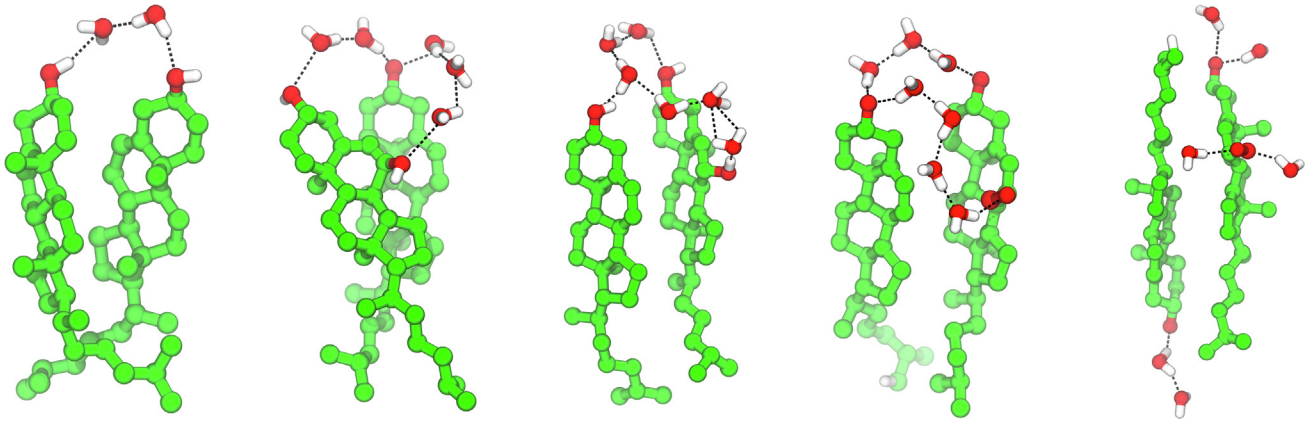

Fig. 16. Chains of H-bonded water molecules linking the polar groups of the molecules in the dimer. From left to right: Chol-Chol; Chol–O7a; Chol–O7b; Chol–OO7a; and Chol–OO7b. The Chol–OO7b dimer has head-to-tail configuration, so the C3-OH groups of the sterols are too far to be linked by H-bonded water molecules.

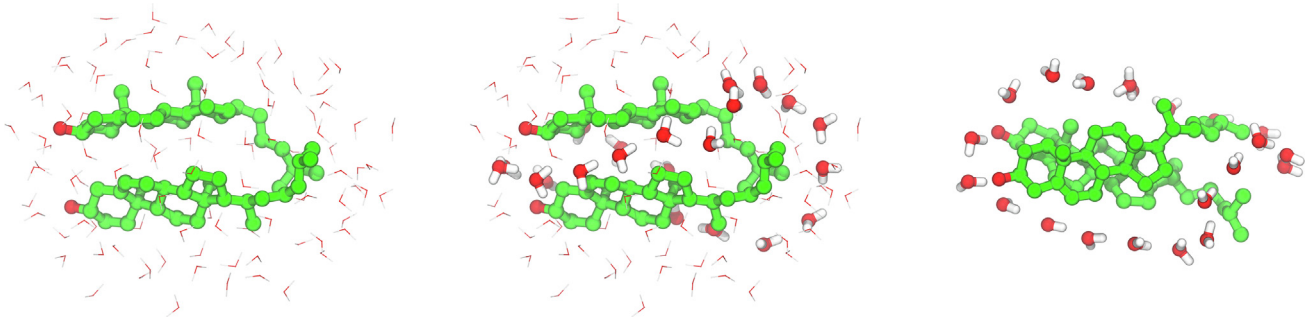

Fig. 17. The distributions of the water molecules from the first hydration shell, *L1*, (*lines*) and from the first cross-layer, *CL1*, (sticks). From left to right: *L1* water of Chol1 and Chol2 – side view; *L1* and *CL1* water – side view; only *CL1* water – top view.

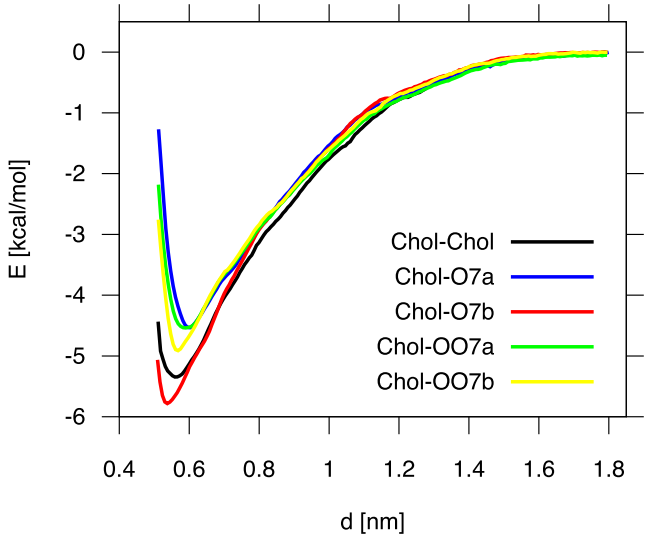

Fig. 18. Potential of mean force profiles as functions of the C13-C13 distance (cf. Section 2.3.2) of Chol-Chol; Chol–O7a; Chol–O7b; Chol–OO7a; and Chol–OO7b dimerisation.

Table 7
The Gibbs free energy change (ΔG) on the formation of a Chol-Chol and Chol-oxChol dimer in water.

Dimer	ΔG [kcal/mol]
Chol–Chol	−5.35 ± 0.13
Chol–O7a	−4.53 ± 0.07
Chol–O7b	−5.78 ± 0.15
Chol–OO7a	−4.54 ± 0.06
Chol–OO7b	−4.91 ± 0.10

oxChol are: 7α-OH-Chol (O7a); 7β-OH-Chol (O7b); 7α-OOH-Chol (OO7a); 7β-OOH-Chol (OO7b). α and β are chiral forms of the hydroxy and hydroperoxy groups, '7′ refers to the C7 carbon atom of the sterol molecule (cf. Fig. 1).

the most stable form of two sterol molecules in water is a dimer. The dimer-water vdW and Coulomb interactions should be similar to the monomer-water interactions (Table 2), but the sterol-sterol vdW interactions that are attractive (Table 6) additionally lower the enthalpic term of ΔG on the dimer formation. On dimerisation, the molecules lose much of their individual motional freedom, however, the dimer as a whole is in a constant motion. This might somewhat compensate for the lost of individual mobility and reduce the entropy decrease on the dimer formation. Again, entropy decrease caused by the dimer-induced reorganisation of the water molecules should be similar to that caused by a monomer. The energetic cost of the release of the water molecules from the contacting surfaces of the molecules on their dehydration can be estimated on the basis of the hydration energy of the Chol molecule. The dehydrated surface constitutes 20% of the whole Chol surface (Fig. 14) and Chol hydration energy is −4.70 kcal/mol (Table 5). Thus, the energy of dehydration of the contacting surfaces of two Chol molecules is ~ 1.9 kcal/mol. However, the released water increases the system entropy and favours dimerisation.

As a more negative value of ΔG implies a stronger association of the molecules in the dimer, one can conclude that the Chol-O7b dimer is the most stable and the Chol-Chol dimer is the next most

stable of the five dimers studied. Also, that dimers of Chol with oxChol in the β form are more stable than their α counterparts (Table 7).

The energy of Chol-Chol attraction in the micelle was evaluated by Gilbert et al. [6] to be within a range of 2 to 4 kcal/mol. The upper value of this range is not far from the value of the free energy gain on Chol dimerisation derived here, of 5.35 kcal/mol (Table 7). On the other hand, the vdW energy of Chol-Chol attraction in the dimer in water is estimated here as ~ -12 kcal/mol (Table 6), whereas Haberland and Reynolds [5] and Gilbert et al. [6] estimated the free energy of micellization as −12.6 kcal/mol. The values obtained in this study and those published in Refs [5,6] are somehow cross-rearranged, although the results of both groups lead to the common conclusion that Chol molecules in the aggregate (dimer) attract each other. Thus, the formation of a Chol-sterol dimer in water is not exclusively due to the hydrophobic effect ("the hydrophobic repulsion by water" as Gilbert et al. say) but also due to the specific intermolecular attractive interactions.

4. Results summary

Cholesterol is an amphipathic molecule with a tiny polar OH group, attached to the carbon atom C3 of a large non-polar part consisting of a tetracyclic ring and a short hydrocarbon chain, attached to the carbon atom C17 (Fig. 1). As such, Chol is insoluble in water but soluble in lipid bilayers. In the body, over 90% of cellular Chol is located in the plasma membrane and, in a much smaller amounts, in intracellular membranes [68–70]. Outside the membrane, Chol aggregates, which is often a cause of pathologic processes, the best recognised of which are the formation of gallstones and atherosclerotic plaque.

The aim of this study is to build a model of the initiation of the atherosclerotic plaque formation which starts from assembling tiny Chol crystals outside the membrane e.g. [1]. Oxidised forms of Chol are also detected in these microcrystals, particularly 7β-OH-Chol, 7-ketocholesterol and 7β-OOH-Chol [31,33,34]. To shed light on the dynamics and energetics of primary nucleation [28] of Chol in water, a model study was undertaken using computational methods. This methodology enables the events leading to molecular self-assembly to be both observed and a detailed analysis of them to be performed. To this end, computer models of one or two sterol molecules in a water box were built, MD simulated and analysed to obtain numerical data elucidating the propensity of Chol and its oxidised forms to associate in water.

The study has two specific goals; one is to obtain basic biophysical information on the sterol-water interactions and the other is to illustrate and elucidate the behaviour of sterol molecules in water and intermolecular interactions that lead to their association which, when it occurs in the human body, might initiate some pathologic process.

The results of the basic biophysical aspect of this study concern the effect of a sterol molecule on the surrounding water molecules, as well as interactions between the sterol and the water on both very short (2 ps) and longer (100 ps) time scales. After a sterol molecule is inserted into a water box, the system equilibrates within ~ 2 ps (Figs. 6, 7, S4 and S5). Water molecules are ordered by both the sterol polar groups, with which they make H-bonds, and by the sterol non-polar part, around which they make a clathrate. For each sterol, the clathrating water exchanges with bulk with a time constant of ~ 7 ps. The time constant of the H-bonded water exchange with bulk depends on the position and chirality of the polar group on the sterol molecule and is ~ 5 ps or ~ 7 ps (Table 4). The free energy calculations indicate that the energy of sterol hydration is negative for all sterols studied and its value depends on the number of the sterol polar groups (Table 5). Similar results were obtained for all amino acids independently of their hydrophobicity [63].

Elucidation of how the contacting areas of two sterol molecules that form a dimer dehydrate (film SF2, SI) can also be considered a basic biophysical result. Nevertheless, this process is crucial to the aggregation of molecules in water, thus is of great relevance to the second aspect of this study.

As dimerization is the first step in the aggregation process, the second specific goal of this study begins from analysing the formation of Chol-Chol and Chol-oxChol dimers. It should be recalled here that the dimer is judged to be formed when Voronoi cells on the surface of one molecule share sides with those of the other molecule which implies that there are no water molecules between the contacting surfaces. Two sterol molecules in water assemble into a dimer rapidly, within the first nanoseconds of MD simulation, and their prevailing configuration, observed in 10 ns of MD simulations, is smooth-rough and head-to-head except for the Chol–7β-OOH-Chol dimer, whose configuration is smooth-smooth head-to-tail. This configuration is also present in the 100-ns MD simulation of the Chol-Chol dimer (Fig. S10, SI). In each dimer, the area of the surface common to both molecules is ~ 1 nm^2, which constitutes ~ 20 % of the total surface area of each molecule. Even though the dimer, once formed, preserves its integrity during the simulations, the arrangement of the molecules is not fixed—the molecules stay together but they are in constant restricted motion and their relative orientation often changes by 180°.

The 100-ns MD simulation of the Chol-Chol dimer in water indicates that a smooth-smooth, head-to-head configuration occurs but is not prevailing. Thus, the arrangement of the molecules in a Chol-Chol dimer in water differs from that in the lipid bilayer, where Chol-Chol dimers are mainly, but not only, in the smooth-smooth and head-to-head configuration [64–66]. Such geometry should be expected because smooth-smooth contact is of low energy and head-to-tail orientation in a lipid bilayer is very improbable. Although the motional freedom of Chol molecules in a lipid bilayer is much more restricted than in water [18], Chol dimers in the bilayer are also dynamic and the dimer itself is not very stable [64,65].

Dehydration of the contacting surfaces on molecular self-assembly had not been intensively studied until recently. The importance of the process in amyloid nucleation is comprehensively discussed in a very recent paper [29]. In the present study, the dehydration of the contacting surfaces of sterols on self-association is analysed using the Voronoi diagram approach and its consecutive steps are illustrated in Fig. 14, S12 and S13 and in film SF2. Dehydration of the interfacial surfaces of associating molecules, formation of the cross-layer water, and growth of the area of the contact surface are all inter-related. The processes occur very fast after the molecules encounter each other, which, on the other hand, is a random event.

The results obtained in this study indicate that the free energy of dimerization is lower for Chol dimers with oxChol in the β than the α form and is the lowest for the Chol–7β-OH-Chol dimer (Table 7). In the 10-ns MD simulation, this dimer has a stable smooth-rough, head-to-head arrangement. One can contemplate whether such orientations of the molecules in the dimer can facilitate and promote the formation of larger sterol oligomers. As high levels of 7β-OH-Chol together with 7-ketocholesterol (which is not studied here) are detected in early and advanced forms of atherosclerotic plaques [31,33], oligomerisation of Chol and some of its oxidised forms certainly takes place. The process of sterol oligomerisation is currently being analysed by us and the formation of trimers and tetramers of sterols in water will be the subject of our next publication.

The arrangement of Chol molecules in liquid-crystalline PC bilayers containing Chol was analysed using computer modelling in Ref. [71]. That study revealed that in the bilayer Chol molecules

are spontaneously packed in such a way that three of them form a triangle around a central molecule. However, the molecules are not in direct contact but are separated from one another by PC acyl chains [71]. In the monohydrate Chol crystal at room temperature the unit cell contains eight Chol molecules in two four-molecule subcells related by twofold symmetry (rotation of 180° coupled with a translation) [15]. The four molecules in the subcell are vertically arranged such that their rings make almost 90° angles with one another [72]. Thus they pack differently from those in the bilayer. At this stage of our study it is not possible to say what the arrangement of Chol molecules in prenucleation clusters [73] is. However, we believe it more likely that the geometry of sterol trimers and tetramers in water is similar to that in the bilayer than in crystal, so possibly they have a triangular-like arrangement. Such geometry may better promote association of subsequent molecules, leading to the formation of the crystal nucleus, and facilitate accommodation the CH_3 and additional polar groups of Chol and oxChol molecules.

Declaration of Competing Interest

The authors declare that they have no known competing financial interests or personal relationships that could have appeared to influence the work reported in this paper.

Acknowledgement

This publication was supported by the Polish National Science Center 2016/22/M/NZ1/00187 (MP-G), by grant R01 EY015526 from the National Institutes of Health, USA (WKS) and in part by PL-Grid Infrastructure.

Appendix A. Supplementary data

Supplementary data to this article can be found online at https://doi.org/10.1016/j.csbj.2021.07.022.

References

[1] Duewell P, Kono H, Rayner KJ, Sirois CM, Vladimer G, Bauernfeind FG, et al. NLRP3 inflammasomes are required for atherogenesis and activated by cholesterol crystals. Nature 2010;464(7293):1357–61.
[2] van Erpecum KJ. Biliary lipids, water and cholesterol gallstones. Biol Cell 2005;97:815–22.
[3] Grebe A, Latz E. Cholesterol Crystals and Inflammation. Curr Rheumatol Rep 2013;15(3):313.
[4] Janoudi A, Shamoun FE, Kalavakunta JK, Abela GS. Cholesterol crystal induced arterial inflammation and destabilization of atherosclerotic plaque. Eur Heart J 2016;37(25):1959–67.
[5] Haberland ME, Reynolds JA. Self-association of cholesterol in aqueous-solution. Proc Nat Acad Sci USA 1973;70(8):2313–6.
[6] Gilbert DB, Tanford C, Reynolds JA. Cholesterol in aqueous-solution – hydrophobicity and self-association. Biochemistry 1975;14(2):444–8.
[7] Loomis CR, Shipley GG, Small DM. The phase behavior of hydrated cholesterol. J Lipid Res 1979;20(4):525–35.
[8] Mainali L, Pasenkiewicz-Gierula M, Subczynski WK. Formation of cholesterol Bilayer Domains Precedes Formation of Cholesterol Crystals in Membranes Made of the Major Phospholipids of Human Eye Lens Fiber Cell Plasma Membranes. Curr Eye Res 2020;45(2):162–72.
[9] Mason RP, Jacob RF. Membrane microdomains and vascular biology – Emerging role in atherogenesis. Circulation 2003;107(17):2270–3.
[10] Raguz M, Mainali L, Widomska J, Subczynski WK. The immiscible cholesterol bilayer domain exists as an integral part of phospholipid bilayer membranes. Biochim Biophys Acta 2011;1808:1072–80.
[11] Mainali L, Raguz M, Subczynski WK. Formation of cholesterol bilayer domains precedes formation of cholesterol crystals in Cholesterol/Dimyristoylphosphatidylcholine membranes: EPR and DSC studies. J Phys Chem B 2013;117(30):8994–9003.
[12] Varsano N, Fargion I, Wolf SG, Leiserowitz L, Addadi L. Formation of 3D cholesterol crystals from 2D nucleation sites in lipid bilayer membranes: implications for atherosclerosis. J Am Chem Soc 2015;137(4):1601–7.
[13] Renshaw PF, Janoff AS, Miller KW. On the nature of dilute aqueous cholesterol suspensions. J Lipid Res 1983;24(1):47–51.
[14] Khaykovich B, Hossain C, McManus JJ, Lomakin A, Moncton DE, Benedek GB. Structure of cholesterol helical ribbons and self-assembling biological springs. P Natl Acad Sci USA 2007;104(23):9656–60.
[15] Craven BM. Pseudosymmetry in Cholesterol Monohydrate. Acta Crystallogr B 1979;35(5):1123–8.
[16] Craven BryanM. Crystal-structure of cholesterol monohydrate. Nature 1976;260(5553):727–9.
[17] Raguz M, Mainali L, Widomska J, Subczynski WK. Using spin-label electron paramagnetic resonance (EPR) to discriminate and characterize the cholesterol bilayer domain. Chem Phys Lipids 2011;164(8):819–29.
[18] Plesnar E, Subczynski WK, Pasenkiewicz-Gierula M. Comparative computer simulation study of cholesterol in hydrated unary and binary lipid bilayers and in an anhydrous crystal. J Phys Chem B 2013;117:8758–69.
[19] Moss GP. Joint Commission on Biochemical Nomenclature. The nomenclature of steroids. Eur J Biochem 1989;186:429–58.
[20] Tangirala RK, Jerome WG, Jones NL, Small DM, Johnson WJ, Glick JM, et al. Formation of cholesterol monohydrate crystals in macrophage-derived foam cells. J Lipid Res 1994;35(1):93–104.
[21] Subczynski WK, Pasenkiewicz-Gierula M. Hypothetical pathway for formation of cholesterol microcrystals initiating the atherosclerotic process. Cell Biochem Biophys 2020;78(3):241–7.
[22] Libby P, Ridker PM, Maseri A. Inflammation and atherosclerosis. Circulation 2002;105(9):1135–43.
[23] Sparrow CP, Parthasarathy S, Steinberg D. A macrophage receptor that recognizes oxidized low-density lipoprotein but not acetylated low-density lipoprotein. J Biol Chem 1989;264(5):2599–604.
[24] Bacellar IOL, Baptista MS. Mechanisms of photosensitized lipid oxidation and membrane permeabilization. ACS Omega 2019;4(26):21636–46.
[25] Štefl M, Šachl R, Olżyńska A, Amaro M, Savchenko D, Deyneka A, et al. Comprehensive portrait of cholesterol containing oxidized membrane. Bba-Biomembranes 2014;1838(7):1769–76.
[26] Olżyńska A, Kulig W, Mikkolainen H, Czerniak T, Jurkiewicz P, Cwiklik L, et al. Tail-oxidized cholesterol enhances membrane permeability for small solutes. Langmuir 2020;36(35):10438–47.
[27] Lee S, Birukov KG, Romanoski CE, Springstead JR, Lusis AJ, Berliner JA. Role of phospholipid oxidation products in atherosclerosis. Circ Res 2012;111(6):778–99.
[28] Rousseau, R. W. Crystallization Processes. in Encyclopedia of Physical Science and Technology (Third Edition) (Meyers, R. A. ed.), Academic Press; 2003, p. 91-119.
[29] Camino JD, Gracia P, Cremades N. The role of water in the primary nucleation of protein amyloid aggregation. Biophys Chem 2021;269.
[30] Brown AJ, Jessup W. Oxysterols and atherosclerosis. Atherosclerosis 1999;142(1):1–28.
[31] Iuliano L. Pathways of cholesterol oxidation via non-enzymatic mechanisms. Chem Phys Lipids 2011;164(6):457–68.
[32] Monier S, Samadi M, Prunet C, Denance M, Laubriet A, Anne AA, et al. Impairment of the cytotoxic and oxidative activities of 7 beta-hydroxycholesterol and 7-ketocholesterol by esterification with oleate. Biochem Bioph Res Co 2003;303:814–24.
[33] Vejux A, Abed-Vieillard D, Hajji K, Zarrouk A, Mackrill JJ, Ghosh S, et al. 7-Ketocholesterol and 7 beta-hydroxycholesterol: In vitro and animal models used to characterize their activities and to identify molecules preventing their toxicity. Biochem Pharmacol 2020;173.
[34] Chisolm GM, Ma G, Irwin KC, Martin LL, Gunderson KG, Linberg LF, et al. 7-beta-hydroperoxycholest-5-En-3-beta-ol, a component of human atherosclerotic lesions, is the primary cytotoxin of oxidized human low-density-lipoprotein. Proc Natl Acad Sci USA 1994;91(24):11452–6.
[35] Hess B, Kutzner C, van der Spoel D, Lindahl E. GROMACS 4: algorithms for highly efficient, load-balanced, and scalable molecular simulation. J Chem Theory Comput 2008;4:435–47.
[36] Abraham MJ, Murtola T, Schulz R, Páll S, Smith JC, Hess B, et al. GROMACS: high performance molecular simulations through multi-level parallelism from laptops to supercomputer. SoftwareX 2015;1-2:19–25.
[37] Jorgensen WL, Maxwell DS, TiradoRives J. Development and testing of the OPLS all-atom force field on conformational energetics and properties of organic liquids. J Am Chem Soc 1996;118:11225–36.
[38] Cornell WD, Cieplak P, Bayly CI, Kollman PA. Application of Resp charges to calculate conformational energies, hydrogen-bond energies, and free-energies of solvation. J Am Chem Soc 1993;115(21):9620–31.
[39] Klauda JB, Garrison SL, Jiang JW, Arora G, Sandler SI. HM-IE: quantum chemical hybrid methods for calculating interaction energies. J Phys Chem A 2004;108:107–12.
[40] Kulig W, Pasenkiewicz-Gierula M, Róg T. Topologies, structures and parameter files for lipid simulations in GROMACS with the OPLS-aa force field: DPPC, POPC, DOPC, PEPC, and cholesterol. Data Brief 2015;5:333–6.
[41] Jorgensen WL, Chandrasekhar J, Madura JD, Impey RW, Klein ML. Comparison of simple potential functions for simulating liquid water. J Chem Phys 1983;79:926–35.
[42] Hess B, Bekker H, Berendsen HJC, Fraaije JGEM. LINCS: a linear constraint solver for molecular simulations. J Comp Chem 1997;18:1463–72.
[43] Essmann U, Perera L, Berkowitz ML, Darden T, Lee H, Pedersen LG. A smooth particle mesh ewald method. J Chem Phys 1995;103:8577–93.
[44] Berendsen HJC, Postma JPM, van Gunsteren WF, DiNola A, Haak JR. Molecular-dynamics with coupling to an external bath. J Chem Phys 1984;81(8):3684–90.

[45] Nosé S. A unified formulation of the constant temperature molecular-dynamics methods. J Chem Phys 1984;81(1):511–9.
[46] Hoover WG. Canonical dynamics: equilibrium phase-space distributions. Phys Rev A 1985;31:1695–7.
[47] Parrinello M, Rahman A. Polymorphic transitions in single-crystals – A new molecular-dynamics method. J Appl Phys 1981;52:7182–90.
[48] McNaught AD, Wilkinson A. Compendium of Chemical Terminology - IUPAC Recommendations (Iupac Chemical Nomenclature Series). The Gold Book. Wiley; 1997.
[49] Chipot C. In: Leimkuhler B et al., editors. Free Energy Calculations in Biological Systems. How Useful Are They in Practice? In: New Algorithms for Macromolecular Simulation. Berlin, Heidelberg: Springer; 2006. p. 185–211.
[50] Liu DC, Nocedal J. On the limited memory Bfgs method for large-scale optimization. Math Program 1989;45(1-3):503–28.
[51] Bennett CH. Efficient estimation of free-energy differences from monte-carlo data. J Comput Phys 1976;22:245–68.
[52] Torrie GM, Valleau JP. Non-physical sampling distributions in monte-carlo free-energy estimation – Umbrella sampling. J Comput Phys 1977;23 (2):187–99.
[53] Stepaniants S, Schulten K, Izrailev S. Extraction of lipids from phospholipid membranes by steered molecular dynamics. J Mol Model 1997;3(12): 473–5.
[54] Kumar S, Bouzida D, Swendsen RH, Kollman PA, Rosenberg JM. The weighted histogram analysis method for free-energy calculations on biomolecules. 1. The Method. J Comput Chem 1992;13:1011–21.
[55] Szczelina R, Murzyn K. DMG-alpha-a computational geometry library for multimolecular systems. J Chem Inf Model 2014;54:3112–23.
[56] Moore EF. In: The shortest path through a maze. Harvard University Press; 1959. p. 285–92.
[57] Agmon N. The grotthuss mechanism. Chem Phys Lett 1995;244(5-6):456–62.
[58] Ropp J, Lawrence C, Farrar TC, Skinner JL. Rotational motion in liquid water is anisotropic: a nuclear magnetic resonance and molecular dynamics simulation study. J Am Chem Soc 2001;123:8047–52.
[59] Rog T, Pasenkiewicz-Gierula M. Non-polar interactions between cholesterol and phospholipids: a molecular dynamics simulation study. Biophys Chem 2004;107:151–64.
[60] Róg T, Murzyn K, Milhaud J, Karttunen M, Pasenkiewicz-Gierula M. Water isotope effect on the phosphatidylcholine bilayer properties: a molecular dynamics simulation study. J Phys Chem B 2009;113(8):2378–87.
[61] Suresh SJ, Naik VM. Hydrogen bond thermodynamic properties of water from dielectric constant data. J Chem Phys 2000;113(21):9727–32.
[62] Zielkiewicz J. Structural properties of water: comparison of the SPC, SPCE, TIP4P, and TIP5P models of water. J Chem Phys 2005;123(10):104501.
[63] Schauperl M, Podewitz M, Waldner BJ, Liedl KR. Enthalpic and Entropic Contributions to Hydrophobicity. J Chem Theory Comput 2016;12(9):4600–10.
[64] Fantini J, Barrantes FJ. How cholesterol interacts with membrane proteins: an exploration of cholesterol-binding sites including CRAC, CARC, and tilted domains. Front Physiol 2013;4.
[65] Bandara A, Panahi A, Pantelopulos GA, Straub JE. Exploring the structure and stability of cholesterol dimer formation in multicomponent lipid bilayers. J Comput Chem 2017;38(16):1479–88.
[66] Elkins MR, Bandara A, Pantelopulos GA, Straub JE, Hong M. Direct observation of cholesterol dimers and tetramers in lipid bilayers. J Phys Chem B 2021;125:1825–37.
[67] Su Yu, Zhou Ao, Xia X, Li W, Sun Z. Quantitative prediction of protein-protein binding affinity with a potential of mean force considering volume correction. Protein Sci 2009;18(12):2550–8.
[68] Goluszko P, Nowicki B. Membrane cholesterol: a crucial molecule affecting interactions of microbial pathogens with mammalian cells. Infect Immun 2005;73(12):7791–6.
[69] Litvinov DY, Savushkin EV, Dergunov AD. Intracellular and Plasma Membrane Events in Cholesterol Transport and Homeostasis. J Lipids 2018;2018:3965054.
[70] Subczynski WK, Pasenkiewicz-Gierula M, Widomska J, Mainali L, Raguz M. High cholesterol/low cholesterol: effects in biological membranes: a review. Cell Biochem Biophys 2017;75(3-4):369–85.
[71] Martinez-Seara H, Róg T, Karttunen M, Vattulainen I, Reigada R, Vij N. Cholesterol Induces Specific Spatial and Orientational Order in Cholesterol/ Phospholipid Membranes. PLoS ONE 2010;5(6):e11162.
[72] Hsu LY, Kampf JW, Nordman CE. Structure and pseudosymmetry of cholesterol at 310 K. Acta Crystallogr B 2002;58:260–4.
[73] Gebauer D, Cölfen H. Prenucleation clusters and non-classical nucleation. Nano Today 2011;6(6):564–84.